

Subduction and slab detachment under moving trenches during ongoing India- Asia convergence

Abdul Qayyum¹, Nalan Lom¹, Eldert L Advokaat², Wim Spakman¹, Douwe G Van Der Meer¹, and D.J.J Van Hinsbergen¹

¹Utrecht University

²University of Birmingham

November 23, 2022

Abstract

The dynamics of slab detachment and associated geological fingerprints have been inferred from various numerical and analogue models. These invariably use a setup with slab-pull-driven convergence in which a slab detaches below a mantle-stationary trench after the arrest of plate convergence due to arrival of continental lithosphere. In contrast, geological reconstructions show that post-detachment plate convergence is common and that trenches and sutures are rarely mantle-stationary during detachment. Here, we identify the more realistic kinematic context of slab detachment using the example of the India-Asia convergent system. We first show that only the India and Himalayas slabs (from India's northern margin) and the Carlsberg slab (from the western margin) unequivocally detached from Indian lithosphere. Several other slabs below the Indian Ocean do not require a Neotethyan origin and may be of Mesotethys and Paleotethys origin. Additionally, the still-connected slabs are being dragged together with the Indian plate forward (Hindu Kush) or sideways (Burma, Chaman) through the mantle. We show that Indian slab detachment occurred at moving trenches during ongoing plate convergence, providing more realistic geodynamic conditions for use in future numerical and analogue experiments. We identify that the actively detaching Hindu Kush slab is a type-example of this setting, whilst a 25-13 Ma phase of shallow detachment of the Himalayas slab, here reconstructed from plate kinematics and tomography, agrees well with independent, published geological estimates from the Himalayas orogen of slab detachment. The Sulaiman Ranges of Pakistan may hold the geological signatures of detachment of the laterally dragged Carlsberg slab.

Hosted file

essoar.10510100.1.docx available at <https://authorea.com/users/544388/articles/601667-subduction-and-slab-detachment-under-moving-trenches-during-ongoing-india-asia-convergence>

1 Subduction and slab detachment under
2 moving trenches during ongoing India-
3 Asia convergence
4

5 Abdul Qayyum^{a*}, Nalan Lom^a, Eldert L. Advokaat^b, Wim Spakman^a,
6 Douwe G. van der Meer^a, Douwe J.J.van Hinsbergen^a
7

8 a Department of Earth Sciences, Utrecht University, Princetonlaan 8a, 3584 CB, Utrecht, the
9 Netherlands

10 b School of Geography, Earth and Environmental Sciences, University of Birmingham, B15 2TT,
11 UK

12
13 *Corresponding author: Abdul Qayyum (geologist.aqayyum@gmail.com)
14

15

16 Abstract

17 The dynamics of slab detachment and associated geological fingerprints have been inferred from
18 various numerical and analogue models. These invariably use a setup with slab-pull-driven convergence
19 in which a slab detaches below a mantle-stationary trench after the arrest of plate convergence due to
20 arrival of continental lithosphere. In contrast, geological reconstructions show that post-detachment
21 plate convergence is common and that trenches and sutures are rarely mantle-stationary during
22 detachment. Here, we identify the more realistic kinematic context of slab detachment using the
23 example of the India-Asia convergent system. We first show that only the India and Himalayas slabs
24 (from India's northern margin) and the Carlsberg slab (from the western margin) unequivocally
25 detached from Indian lithosphere. Several other slabs below the Indian Ocean do not require a
26 Neotethyan origin and may be of Mesotethys and Paleotethys origin. Additionally, the still-connected
27 slabs are being dragged together with the Indian plate forward (Hindu Kush) or sideways (Burma,
28 Chaman) through the mantle. We show that Indian slab detachment occurred at moving trenches during
29 ongoing plate convergence, providing more realistic geodynamic conditions for use in future numerical
30 and analogue experiments. We identify that the actively detaching Hindu Kush slab is a type-example
31 of this setting, whilst a 25-13 Ma phase of shallow detachment of the Himalayas slab, here reconstructed
32 from plate kinematics and tomography, agrees well with independent, published geological estimates
33 from the Himalayas orogen of slab detachment. The Sulaiman Ranges of Pakistan may hold the
34 geological signatures of detachment of the laterally dragged Carlsberg slab.

35

36 1. INTRODUCTION

37 If negative buoyancy of subducted lithosphere pulling slabs into the mantle is the prime driver of
38 plate tectonics, as widely thought (Conrad & Lithgow-Bertelloni, 2002; Forsyth & Uyedat, 1975;
39 Lithgow-bertelloni & Richards, 1998a), the detachment of a slab from a surface plate is a key event to
40 calibrate the drivers of plate motion (Fernández-García et al., 2019; van Hunen and Allen, 2011;
41 Bercovici et al., 2015; Duretz et al., 2011). Because slab detachment occurs at depth and is not an
42 instantaneous process it cannot be directly constrained from geophysical or geological observations
43 (Duretz et al., 2014; van Hunen & Allen, 2011; Wortel & Spakman, 2000). For that reason snap shot
44 observations from e.g., seismic tomography, or earthquake focal mechanisms, in regions where the
45 process may be presently active (e.g., the Hindu Kush (Kufner et al., 2017), the southern Banda Arc
46 (Ely & Sandiford, 2010), the south-eastern Carpathians (Sperner et al., 2001), or the central-eastern
47 Betics (Spakman et al. 2018) are complemented with inferences made from numerical and analogue

48 experiments. For those experiments, however, it is important to first identify if they can represent the
49 natural example under investigation.

50 Earliest analogue and numerical experiments (Buitter et al., 2002; Buitter & Pfiffner, 2003;
51 Chemenda et al., 1995; Taras V. Gerya et al., 2004; Yoshioka & Wortel, 1995; van de Zedde & Wortel,
52 2001) were designed to evaluate whether slab detachment would be a physically plausible explanation
53 for geological observations such as transient surface uplift, heating, and magmatism, in regions where
54 seismological inference suggests that a slab has broken off (Davies & von Blanckenburg, 1995; Maury
55 et al., 2002; van der Meulen et al., 1998; Wortel & Spakman, 1992, 2000). Subsequent models have
56 become more advanced and were expanded to 3D (Duretz et al., 2014; Duretz et al., 2011; van Hunen
57 & Allen, 2011; Regard et al., 2008; Yoshioka & Wortel, 1995). Dynamic transient topographic changes,
58 high-temperature metamorphism, and magmatism have since become widely used as signature events
59 to date suspected slab break-off phases (Atherton & Ghani, 2002; Kohn et al., 2002; Zhen Li et al.,
60 2014; Maheo et al., 2002; Vissers et al., 2016; Yuan et al., 2010). However, as Garzanti et al. (2018)
61 recently wrote: “slab breakoff has been invoked in so many settings and time frames that it could have
62 hardly taken place in each and every case in which it was called upon”. In other words, the geological
63 observations that are widely considered as signatures of slab detachment are likely equivocal and cannot
64 be called unique identifiers of the process.

65 Importantly, models of slab detachment published so far invariably assume a very specific geodynamic
66 setting involving a mantle stationary trench at which plate convergence as well as absolute plate motion
67 come to halt when continental lithosphere enters the trench (e.g., Duretz et al., 2011; van Hunen &
68 Allen, 2011; van de Zedde & Wortel, 2001). After this, the hanging and steepening slab gradually
69 detaches by shearing and necking (e.g., Duretz et al. 2012) due to the still active slab pull. Following
70 detachment the detached slabs sink vertically below the mantle-stationary suture (Figure 1)
71 (Běhounková & Čížková, 2008; Billen, 2010; Duretz et al., 2011; Gerya et al., 2004; González &
72 Negredo, 2012; van Hunen & Allen, 2011; Lee & King, 2011). In contrast, in- almost all natural cases
73 where slab detachment occurred in the last tens of millions of years, plate convergence continued long
74 after detachment. In addition, the trenches at which detachment occurred, as well as the upper and lower
75 plates, kept moving relative to the mantle (Agard et al., 2011a; Hafkenscheid et al., 2006; van
76 Hinsbergen et al., 2019, 2020a; van de Lagemaat et al., 2018; Parsons et al., 2020; Schellart & Spakman,
77 2015), consequently leading to suture zones across the globe that are typically offset relative to their
78 corresponding, detached slabs (Domeier et al., 2016; van der Meer et al., 2010; 2018; Schellart &
79 Spakman, 2015; Vissers et al., 2016). Therefore, if the process of slab detachment occurs while relative
80 and absolute plate motion is ongoing, this may influence the dynamics of the process and perhaps may
81 entail different geological responses than inferred from the detachment modelling so far.

82 A prime example where slab detachment occurred during ongoing plate convergence is at
83 subduction zone(s) that consumed Indian plate lithosphere during convergence with Asia.
84 Seismological studies have revealed that (except for the far north-western corner in the Hindu Kush,
85 Kufner et al., 2017) there is currently no subducting slab attached to northern India (Agius & Lebedev,
86 2013; Chen et al., 2017; Nábelek et al., 2009; Replumaz et al., 2010; Van Der Voo et al., 1999), yet
87 thousands of km of India-Asia convergence occurred since Cretaceous time and must have been
88 accommodated by subduction (Molnar & tapponnier, 1975; Patriat & Achache, 1984). Even today, the
89 absolute northward Indian plate motion and relative India-Asia convergence continues, with a steady
90 northward pace that has been ~4 cm/a for the last 13 Ma (Copley et al., 2010; DeMets & Merkouriev,
91 2021; van Hinsbergen et al., 2011; Molnar & Stock, 2009).

92 The mantle below India and Indian Ocean was among the first regions where deep mantle
93 structure was correlated to subduction history (Hafkenscheid et al., 2006; Replumaz et al., 2004; Van
94 Der Voo et al., 1999). These studies identified multiple detached slabs, and the shallowest of these are
95 identified hundreds to more than 1500 km to the south of the modern northern extent of the Indian
96 continental lithosphere which is imaged sub-horizontally below Tibet over a distance of 300-800 km
97 north of the modern plate boundary, the southern Himalayan front (Agius & Lebedev, 2013; Chen et
98 al., 2017; van Hinsbergen et al., 2019) (Figure 2). Clearly, these geodynamic constraints differ
99 completely from those used for the past numerical models simulating slab detachment and from which
100 the currently perceived diagnostic geological signatures of slab detachment are derived.

101 In this paper, we aim to investigate the kinematic history of slab detachment events during ongoing
102 Indian plate subduction and convergence. To this end, we first need to evaluate which of the previously
103 identified anomalies are likely representing subducted (Neotethyan) lithosphere that detached from the
104 Indian plate, rather than from older plates whose relics are now found in Tibet. Ever since the first
105 interpretation of van der Voo et al. (1999) all lithosphere below India has been interpreted as
106 Neotethyan oceanic lithosphere that detached from the Indian continental margin since the Cretaceous.
107 However, global correlations between slabs and geological records have since then shown that
108 anomalies in the deep mantle may represent slabs that subducted in the Permo-Triassic and Jurassic
109 (van der Meer et al., 2010; 2018; Sigloch & Mihalynuk, 2013). Part of the slabs below the Indian Plate
110 that were previously interpreted as Neotethyan may thus well relate to earlier, Permo-Triassic to Early
111 Cretaceous subduction of which the corresponding geological records are located in the Mesozoic
112 geology of accreted blocks that are now found in the Tibetan Plateau. From the anomalies that are most
113 likely Neotethyan, we then evaluate previous estimates of the timing of detachment from the Indian
114 plate and evaluate to what extent the conditions under which detachment occurred, differ from classical
115 concepts. Finally, we evaluate the effects that ongoing motion during slab detachment may conceptually
116 have on the mechanism of detachment, evaluate whether the detachment events may have first-order
117 expressions in the geological record, and determine a set of geodynamic conditions and case study areas

118 for future modelling experiments to evaluate what geological observations may be diagnostic for slab
119 detachment while the slab is be dragged by, and in the direction of the absolute motion of the lower
120 plate.

121

122 2. Identifying Neotethyan subducted slabs below India

123 2.1 Context: global correlations between seismic tomography and geology

124 With the development of global seismic mantle tomography towards more detailed imaging of
125 slabs and their remnants, now some 25 years ago (Bijwaard et al., 1998; van der Hilst et al., 1997; Grand
126 et al., 1997), came the opportunity to infer the current deep mantle locations of lithosphere that once
127 subducted at still-active, or former and now inactive paleo-subduction zones. In the ten years prior,
128 upper mantle slabs had been correlated to mostly active subduction zones e.g., (Fukao et al., 1992; Hilst
129 et al., 1991; Spakman et al., 1988), and the first lower-mantle anomalies became correlated to subducted
130 oceanic lithosphere predicted by plate reconstructions in the Tethyan and Pacific realms (Duretz et al.,
131 2014; Fukao et al., 2001; Grand et al., 1997; Hafkenscheid et al., 2006; van Hinsbergen et al., 2005;
132 Lippert et al., 2014; Lithgow-Bertelloni & Richards, 1998b; Replumaz & Tapponnier, 2003; Richards
133 & Engebretson, 1990; Van Der Voo et al., 1999). A next development was the reconstruction of the
134 ‘mantle memory’ of subduction through systematic correlation between remnants of detached slabs in
135 the mantle and locations of paleo-subduction in plate tectonic reconstruction models (van der Meer et
136 al., 2010). This revealed that increasingly deeper slabs tend to be well-explained by increasingly older
137 subduction zones, with Cenozoic subduction mostly restricted to the upper mantle, and top of the lower
138 mantle, and slabs on the core-mantle boundary correlating to Permo-Triassic slabs (Butterworth et al.,
139 2014; Domeier et al., 2016; van der Meer et al., 2010; 2018; Sigloch & Mihalynuk, 2013). The
140 correlations moreover showed that in general, detached sinking slabs do not tend to move laterally
141 relative to each other (van der Meer et al., 2018), and sink more or less vertically through the mantle
142 (Domeier et al., 2016).

143 In contrast, slabs can and do move laterally through the mantle when they are still attached to
144 surface plates, as suggested by the reconstructions of moving trenches in absolute plate motion models
145 (Hall & Spakman, 2002; van de Lagemaat et al., 2018; Lallemand et al., 2008; Parsons et al., 2021;
146 Schellart, 2008; Schellart & Spakman, 2015; Sdrolias & Müller, 2006). Sigloch and Mihalynuk (2013)
147 argued that the shape of slabs imaged in seismic tomography contains valuable information on the
148 absolute motion that their corresponding trenches underwent during subduction. Schepers et al. (2017)
149 and Boschman et al. (2018) slightly modified this concept to include effects of periods of flat slab
150 subduction and argued that slab shape reflects the absolute motion of the location where the slab bended
151 into the mantle during its subduction, whereby the slab bend and trench may be offset by a flat slab

152 segment that may vary in width through time. These concepts predict that during subduction with
153 mantle-stationary slab bends, slabs tend to form near-vertical walls of thickened/folded slab in the
154 mantle transition zone while sinking into the lower mantle (Figure 4a-c). At retreating slab bends (i.e.
155 roll-back), however, slabs tend to drape on the 660 km discontinuity and become flat-lying (e.g., van
156 der Hilst et al. 1993) (Figure 4 d-f). Advancing slab bends lead to overturned slabs (Figure 4g-i)(van
157 Hinsbergen et al., 2019; Van Der Voo et al., 1999). These flat-lying slabs will eventually also sink
158 vertically through the mantle while maintaining their shape (Boschman et al., 2018), causing that their
159 average sinking rate from the moment of detachment tends to be reduced as compared to slabs sinking
160 below a mantle-stationary trench (van der Meer et al. 2018). A current example is the Izu-Bonin slab
161 that is subducting at a retreating part of the Izu-Bonin-Marianas trench and that is mostly overlying the
162 660 km discontinuity (e.g. van der Hilst et al. 1993; van der Hilst and Seno 1993), whereas in the south
163 where the trench has been more mantle-stationary, the Marianas slab reached as deep as 1200 km (van
164 der Hilst and Seno 1993; Miller et al., 2005; Wu et al., 2016). Moreover, while actively subducting
165 slabs may be dragged sideways by the absolute motion of the downgoing plate at the trench, over
166 distances in excess of 1000 km (van de Lagemaat et al., 2018; Parsons et al., 2021; Spakman et al.,
167 2018) implying that the modern location of slab remnants in the mantle is a reasonable marker for where
168 slabs detached, but not necessarily where they started their subduction.

169

170 2.2 Geological constraints on ocean closure in Tibet

171 We aim to identify the location and shape of slabs that detached from the Indian plate during its
172 northward motion towards Eurasia since the Early Cretaceous. The relationships summarized above
173 then require that we distinguish these Cretaceous and younger slabs from other slabs that were
174 subducted in Permo-Triassic to Early Cretaceous time that globally tend to be in the lower to mid-
175 mantle(van der Meer et al., 2018; van Der Meer et al., 2010), depending on their history of subduction.

176 The geological record of Tibet and the Himalayas shows evidence for multiple subduction zones
177 that have been active at times between the Permian times to the present zones (Figure 2,3,8). The
178 youngest record of subduction and accretion in the system is the Cenozoic Himalayan accretionary
179 orogen, which forms an incomplete, thrust, and often metamorphosed record of continent-derived,
180 mostly sedimentary units stripped off their subducted or otherwise deep under thrust lower crustal
181 and mantle lithospheric underpinnings (van Hinsbergen & Schouten, 2021; Hodges, 2000; Kapp &
182 DeCelles, 2019). The Himalayas is bounded to the north by the Indus-Yarlung (Tsangpo) suture zone
183 with relics of Triassic '*Neotethys*' ocean floor that subducted northward since at least Early Cretaceous
184 time (~130 Ma) below the Lhasa terrane of southern Tibet (Hébert et al., 2012; Kapp and Decelles,
185 2019; Maffione et al., 2015). In this time interval (since at least Early Cretaceous time) the net amount
186 of convergence between India and Asia was ~8000 km (Figure 3). Tibetan shortening started already

187 in Cretaceous time and amounted a few hundred kilometres (van Hinsbergen et al., 2011; Kapp et al.,
188 2005; Murphy et al., 1997) and between ~50 Ma and the present, Tibetan shortening, in the east aided
189 by extrusion of Indo-China, led to ~1000-1200 km of northward indentation of the India-Eurasia plate
190 boundary (Replumaz & Tapponnier 2003, Royden *et al.* 2008, van Hinsbergen *et al.* 2011, 2019; Ingalls
191 *et al.* 2016), and a minimum of ~6500-7000 km of lithosphere must this have been consumed by
192 subduction. Seismic tomography studies have shown that at present, Indian continental lithosphere lies
193 horizontally directly below southern Tibetan crust, and thus interpreted that mantle lithosphere that
194 originally underpinned Tibetan crust must have been lost to delamination (Nábelek et al., 2009). This
195 delaminated lithosphere may thus also contribute to, presumably small-scale, seismic velocity
196 anomalies below Tibet (Replumaz et al., 2013).

197 The Lhasa terrane is separated by the Bangong-Nujiang suture from the Qiangtang terrane
198 (Figure 2). The geological record of the suture zone, as well as paleomagnetic constraints from the
199 Lhasa and Qiangtang terranes, reveal that this suture accommodated the closure of a once ~6000 km
200 wide '*Mesotethys*' ocean between the late Triassic and early Cretaceous (Figure 3,8) (Kapp & Decelles,
201 2019; S. Li et al., 2019; Zhenyu Li et al., 2016; Yin & Harrison, 2000). Contemporaneous arc magmatic
202 rocks on both sides of the suture zone, and the structure of the suture zone itself, have been interpreted
203 to show that closure of the Mesotethys ocean was likely accommodated by double sided subduction
204 (Luo & Fan, 2020; Zhu et al., 2016). Alternatively, Kapp and DeCelles (2019) inferred that all
205 magmatism on Lhasa since the Triassic resulted from northward Neotethys subduction along its
206 southern margin and that Mesotethys closure was entirely accommodated by northward subduction
207 below Qiangtang.

208 The Qiangtang terrane is separated from NE Tibetan terranes by the Songpan-Garzi accretionary
209 prism (Figure 2) that consists mostly of accreted Permo-Triassic clastic sedimentary rocks thought to
210 have derived from subducted '*Paleotethys*' ocean floor. Paleomagnetic data show that the Paleotethys
211 was of similar width as the Meso- and Neotethys, on the order of 6000 km, and closed throughout the
212 Permo-Triassic time (Figure 3) (Song et al., 2017). Contemporaneous arcs on either side of the
213 subduction zone, and tectonic architecture show that also this closure was likely associated with double-
214 sided subduction (Kapp & Decelles, 2019). Sutures within NE Tibet predate the Mesozoic and predate
215 the reconstructed mantle memory (van der Meer et al., 2018). These terranes have moved together with
216 the North China block since Paleozoic time, until late Cenozoic shortening during Tibetan plateau
217 growth (Wu et al., 2016; Yin & Harrison, 2000).

218 Based on global correlations between slabs and geologically reconstructed subduction zones
219 (Butterworth et al., 2014; van der Meer et al., 2010; 2018; Sigloch & Mihalynuk, 2013), we expect that
220 slabs related to Paleotethys, Mesotethys, and Neotethys subduction are still visible in the mantle. And
221 because the three oceans had similar width (Figure 3), the associated seismic velocity anomalies are

222 expected to have roughly similar volumes, if there was no additional crustal production from mid-
223 ocean-ridge spreading. We use this as a guide in our interpretation: variations in volume may also be
224 due to differences in tomographic resolution, resolved seismic velocity amplitudes (Hafkenscheid et al.
225 2006) and volume changes as result of compression and phase changes during sinking into the deep
226 mantle (Van Der Meer et al., 2014).

227 The closure of one ocean basin may be accommodated by multiple slabs, as has been argued for
228 Mesotethys and Paleotethys closure (see above). Reconstructions of Neotethys subduction history
229 include models that interpret (i) a single subduction zone that remained more or less mantle-stationary
230 along southern Tibet since the Early Cretaceous (van Hinsbergen et al., 2019), (ii) a single subduction
231 zone that rolled back from the Tibetan margin to an equatorial position in the Cretaceous that came to
232 an arrest during Late Cretaceous (Hafkenscheid et al., 2006) or Paleocene (Kapp & Decelles, 2019)
233 arrival of the Indian margin in the trench, followed by renewed subduction along the Eurasian margin;
234 (iii) a double subduction zone including one along southern Tibet and an intra-oceanic one that started
235 in the Early Cretaceous at the equator and that remained active at the until Cretaceous or Eocene arrival
236 of India in the trench (Tapponnier et al., 1981; Aitchison et al., 2007, van Hinsbergen et al., 2012), or
237 advanced towards the south Tibetan margin in the Eocene (Jagoutz et al., 2015; Martin et al., 2020).
238 The latter scenario suggests that even though subduction started at the equator, the slab was dragged
239 northward through the mantle during subduction and detached close to the southern Eurasian margin.
240 Interpretations of when continental lithosphere arrives at the south Tibetan trench vary considerably
241 (see overview in e.g., (Parsons et al., 2020), but only impact the type of lithosphere that is consumed
242 by subduction and underthrusting, but not the amount, and the differences in collision age between these
243 models are hence not of importance to our kinematic analysis and tomographic interpretation.

244 Finally, the geological record and plate reconstructions reveal evidence for west- and east-ward
245 subduction of Indian plate lithosphere during India's northward flight. Westward subduction is
246 reconstructed and documented from the Sulaiman ranges orogen and overlying ophiolites in Pakistan
247 and occurred from ~70 Ma until the Eocene, followed by oblique underthrusting of west India below
248 Eurasia occurred in the Neogene (Gaina et al., 2015; Gnos et al., 1998). The latter deformation is
249 partitioned over the Sulaiman ranges fold-thrust belt and the left-lateral Chaman Fault that together
250 form the western plate boundary of Indian plate (Figure 2). To the east, subduction occurred below the
251 Andaman Islands and the West Burma Block since the Cretaceous (Plunder et al., 2020; Westerweel et
252 al., 2019; Bandopadhyay et al., 2021), and became increasingly more oblique upon northward migration
253 of the India-Asia plate boundary due to shortening in Tibet (van Hinsbergen et al., 2011; 2019). Also
254 here, deformation is partitioned over a frontal fold-thrust belt (the Indo-Burman ranges and the
255 Andaman-Nicobar accretionary wedge) and a transform system (the right-lateral Sagaing-Andaman
256 Sea-Sumatran Fault system) (e.g., Morley & Arboit, 2019) (Figure 2).

257

258

259 2.3. Absolute plate motions: where to search and what to search for?

260 Searching for the anomalies that correspond to the closure of the Tethyan oceans requires
261 constraints on absolute plate motion (i.e., relative to the mantle) of India and Asia. True polar wander-
262 corrected paleomagnetic reference frames suggest that Eurasia did not move appreciably in absolute
263 latitude since the Jurassic (Torsvik et al., 2012), and when adding paleomagnetism-based pre-
264 Cretaceous reconstructions of North China (and Tibetan units accreted to that) relative to Siberia, the
265 absolute paleolatitude of Tibet is about latitudinally stable before that time as well (Torsvik et al., 2012;
266 Van Der Voo et al., 2015; Torsvik and Cocks, 2017)(Figure 3). Absolute plate motions back to
267 Cretaceous time are reasonably well constrained by hotspot reference frames (Dobrovine et al., 2012;
268 Torsvik et al., 2019). Prior to the Cretaceous, paleolongitudinal control is more challenging, but global
269 correlations between subduction zones and slabs (Van der Meer et al., 2018; Van Der Meer et al., 2010)
270 , or between intraplate volcanics correlated to stationary plume-generation-zones at the core-mantle
271 boundary (Burke et al., 2008; Torsvik et al., 2014) suggest that Eurasia also did not move much in
272 paleolongitude since the Triassic. Consequently, assuming vertical sinking of slab remnants, the
273 lithosphere that was consumed by Paleo-, Meso-, and Neotethys subduction is generally expected to be
274 still located below the Indian plate and Tibet today (Hafkenscheid et al., 2006; van der Meer et al.,
275 2018; Parsons et al., 2020; Van Der Voo et al., 1999).

276 With Eurasia as more or less mantle-stationary, the Tethyan oceans closing during absolute
277 northward motion of plates carrying the (micro-)continents of Qiangtang, Lhasa, and India, and using
278 the subduction polarities interpreted from geology as summarized above, we may predict mantle
279 structure that results from the various scenarios using the relationship between absolute trench motion
280 and resulting slab geometry. Southward subduction below the Qiangtang and Lhasa terranes during
281 their northward flights in the Permo-Triassic, and Triassic-Early Cretaceous, respectively, should have
282 been associated with slab roll-back and predict flat-lying slabs of a few thousand km wide below much
283 of the Indian Plate. If subduction was northward below the Lhasa terrane during its northward motion
284 (Kapp & Decelles, 2019), the trench would have advanced and a flat-lying slab is also expected,
285 although this slab would be overturned. Northward subduction of the Paleotethys below NE Tibet and
286 of the Mesotethys below Qiangtang would have formed slab walls. Near-stationary Neotethys
287 subduction below southern Tibet in Cretaceous to Eocene time would generate a slab wall, whereas the
288 ~1000 km of northward trench advance associated with Tibetan shortening since the Eocene would
289 result in overturned and flat(ter) lying slabs if lithosphere subducted, and/or horizontally underthrust
290 lithosphere below Eurasia, if deep subduction was prohibited by excess buoyancy of the underthrusting
291 lithosphere. Equatorial subduction preceded by slab retreat (Hafkenscheid et al., 2006; Kapp &

292 Decelles, 2019) or followed by slab advance (Jagoutz et al., 2015; Martin et al., 2020) would lead to
293 flat-lying slabs south of the main slab wall of south Tibetan subduction, whereas mantle-stationary
294 equatorial subduction in the Neotethys (Tapponnier et al., 1980; Aitchison et al., 2007; van Hinsbergen
295 et al., 2012) would produce a second slab wall along-side the one forming along southern Tibet (Figure
296 8). Finally, slabs that subducted west and east of India in Cretaceous to Cenozoic time must have
297 undergone northward, more or less slab-strike parallel dragging as long as they were attached to the
298 moving Indian lithosphere, or should have been left behind and sinking vertically at the location of their
299 detachment (Le Dain et al., 1984; van de Lagemaat et al., 2018; Parsons et al., 2021; Spakman et al.,
300 2018).

301

302 3. Seismic tomographic constraints on mantle structure

303 3.1 Approach

304 The first study of seismic tomographic images of the mantle below India and Tibet was conducted
305 by van der Voo et al. (1999). Together with subsequent studies about a dozen anomalies have now been
306 identified (Hafkenscheid et al., 2006; van der Meer et al., 2010; 2018; Negrodo et al., 2007; Parsons et
307 al., 2020; Replumaz et al., 2010; 2014). The number of tomographic anomalies in the mantle below
308 India and Tibet is far greater than the number of ocean basins that was consumed, from which it follows
309 that there are more slab detachment phases than continental collisions.

310 The initial studies of van der Voo et al. (1999), Replumaz et al. (2004), and Hafkenscheid et al.
311 (2006) assumed that all slabs below southern Tibet and India represented Neotethyan lithosphere that
312 subducted in Cretaceous and younger time. Only subducted slabs in the lower mantle below Tibet, to
313 the north of the Indus-Yarlung suture between India and Asia, were interpreted by these authors as
314 relicts of the Mesotethys or Paleotethys oceans that subducted before Early Cretaceous time (Figure
315 2,8). Even though in the decade that followed global tomography-geology connections have shown that
316 also Triassic and Jurassic subducted slabs are typically still visible in the lower mantle (van der Meer
317 et al., 2010; 2018; Sigloch & Mihalynuk, 2013) all studies of anomalies in the mantle below India still
318 assume all of these are Neotethyan (Parsons et al., 2020).

319 As basis for our re-evaluation of Tethyan slabs, we use the nomenclature of slabs as defined in
320 the Atlas of the Underworld compilation of tomographic anomalies of van der Meer et al. (2018), which
321 includes all anomalies that had previously been interpreted as subducted slabs. This nomenclature
322 names anomalies after presently overlying geographic features instead of after the lithosphere/basin that
323 they are interpreted to represent. This objectively labels the anomalies and leaves freedom for
324 interpretation. We refer the reader to this document for names that have been used by previous workers
325 and note that Parsons et al. (2020) recently labelled these anomalies differently.

326 In addition to the compilation of van der Meer et al. (2018), we include one previously identified
327 anomaly below Tibet described by Replumaz et al. (2013) (their AF anomaly that they interpreted as
328 delaminated Tibetan lithosphere rather than a subducted slab) and identify several anomalies that have
329 not previously been described, in the shallow upper mantle and in the deepest lower mantle. We use the
330 UU-P07 P-wave tomographic model (Amaru, 2007; Hall & Spakman, 2015) that was also used by van
331 der Meer et al. (2018), and in addition analyse vote maps (Shephard et al., 2017) to evaluate the
332 occurrence of the identified anomalies across tomographic models (Figure 2, Figure 3). In the following
333 paragraphs, we navigate through mantle structure below India and Tibet from the largest anomaly that
334 has so far been interpreted as the main body of Neotethyan lithosphere, and from there correlate
335 shallower and deeper slabs as Neotethyan, Mesotethyan, and Paleotethyan slabs.

336

337 3.2 Slabs below India and Tibet and their previous interpretations

338 The most prominent tomographic anomaly in the mantle below India is the *India slab* (Figure
339 5,6). In the west, the India slab is found around 700-1600 km depth, becomes deeper (1000-1800 km)
340 below central India, and shallower again towards the east (700-1600 km). It has a N-S width of up to
341 1500 km suggesting major thickening. The anomaly is striking NW-SE (Figure 5,6), at the location
342 where in the mantle frame of reference (Dobrovine 2012) the southern Tibetan active margin is
343 restored in Cretaceous to Eocene time (van Hinsbergen et al., 2019; Replumaz et al., 2004; Royden et
344 al., 2008). Ever since its first identification by van der Voo et al. (1999), the India anomaly has
345 consistently been interpreted as the main body of Neotethyan lithosphere that subducted at a trench
346 along the Cretaceous to Paleogene south Tibetan margin. The India slab is overall more or less vertically
347 aligned as a slab wall (Sigloch & Mihalynuk, 2013). Tectonic reconstructions supported by
348 paleomagnetic data and placed in a mantle frame of reference (Dobrovine et al., 2012) suggest that
349 this trench advanced over some 500 km during the late Cretaceous to early Eocene (van Hinsbergen et
350 al., 2019; Lippert et al., 2014). This advance is likely too small to be tomographically detected in the
351 blurred image of the thickened/buckled slab remnant. The vertical extent of the slab is an order of
352 magnitude smaller than the amount of early Cretaceous to Eocene India-Asia convergence, and if this
353 slab hosts the main body of Neotethyan lithosphere, it must have thickened, e.g., by buckling and/or
354 lateral spreading. At peak convergence rates in excess of 20 cm/a (DeMets & Merkouriev, 2021), may
355 have contributed to thickening upon entering the lower mantle.

356 To the north of the India slab, at a shallower depth of 400-800 km, the *Himalayas slab* is found
357 (HM: Figure5,7). Along-strike, the slab varies in orientation from vertical to south-dipping, the latter
358 interpreted as an overturned orientation (Replumaz et al., 2010). The Himalayas slab is at its largest,
359 and its base is at its deepest, below the central part of the Indian continent and becomes shallower
360 towards the east and west. The shallowest part of top of the Himalayas slab is located below the central-

361 eastern Himalayas (Figure 5,6). The Himalayas slab is detached and offset northward from the Indian
362 slab even though it is interpreted to have subducted below southern Tibet along Himalayan thrusts (
363 Van Hinsbergen et al., 2012; Parsons et al., 2021; Replumaz et al., 2010). Its overturned position and
364 northward offset relative to the Indian plate are interpreted to reflect subduction during northward trench
365 advance accommodated by Cenozoic shortening and extrusion in the Tibetan plateau (van Hinsbergen
366 et al., 2019; Replumaz et al., 2010). This slab is interpreted to be the youngest slab to have detached
367 from the northern Indian margin (Replumaz et al., 2010; 2004).

368 The northern margin of *Indian plate lithosphere* that is horizontally underthrust directly below
369 the Tibetan Plateau crust (Chen et al., 2017; Nábelek et al., 2009) protrudes northward from the
370 Himalayan thrust front, over a distance that varies along strike from ~800 km near the syntaxes, to ~400
371 km from the east-central Himalayas to the north (Agius & Lebedev, 2013; van Hinsbergen et al., 2019).
372 The northern edge of this horizontally underthrust lithosphere is offset northward from the detached
373 Himalayas slab (Figure 6), which must reflect the amount of absolute northward motion of the Indian
374 plate after detachment (van Hinsbergen et al., 2019).

375 Below the Hindu Kush, to the west of the western Himalayan syntaxis, the *Hindu Kush* slab is
376 located (HK: Figure 5). The slab is interpreted as oceanic lithosphere that is still attached to the north-
377 western Indian continental margin, but that lies buried below the Sulaiman Ranges of Pakistan (Kufner
378 et al., 2017). It is a N-dipping, E-W trending, near-vertical anomaly that reaches a depth of ~600 km
379 below Hindu Kush region in North Pakistan (Kufner et al., 2017; C. Li & Hilst, 2010; Negredo et al.,
380 2007; Replumaz et al., 2010; Van Der Voo et al., 1999) and is offset northward relative to the Himalayas
381 slab by a few hundred km (Figure 2). Detailed seismological studies have shown that the slab is
382 currently in the process of detaching (Kufner et al., 2017, 2021; Lister et al., 2008).

383 In the east, the *Burma slab* is imaged as a N-S striking, steeply-east-dipping anomaly under the
384 west Burma Block of Myanmar, still connected to the northward moving Indian plate (Figure 5,7).
385 This upper mantle slab has been recognized in many earlier studies and is disconnected by a slab
386 window below the Andaman Sea from the Sunda slab below Sumatra and Java (Huang and Zhao,
387 2006; Li et al., 2008; Replumaz et al., 2010; Zhao and Ohtani, 2009; Parsons et al., 2021). The Burma
388 slab has accommodated the E-W convergence component of the highly oblique subduction between
389 India and Sundaland (Figure 2), which amounted ~600 km since ~40 Ma (van Hinsbergen et al.,
390 2011). A mirror image of the Burma slab, identified for the first time here, is formed by the *Chaman*
391 *slab* to the west of India (CS; Figure 5,7), dipping westward below the Helmand Block and Chaman
392 Fault of Afghanistan and Pakistan. The Chaman slab may still be connected to the western margin of
393 India and is imaged down to a depth of ~500-600 km (Figure 5,7).

394 The Chaman slab is separated from and offset northward relative to the *Makran slab* (MK; Figure
395 5,7). Even though subduction below the Makran and the resulting formation of the major Makran

396 accretionary prism is well-known (Byrne et al., 1992; Kopp et al., 2000; Yamini-Fard et al., 2007),
397 seismic tomographic images of the Makran slab are rare. Hafkenscheid et al. (2006) showed one cross
398 section in the western Makran that reveals an upper mantle slab that is decoupled from deeper, lower
399 mantle anomalies, but did not explicitly identify this anomaly as a slab, which we do here, to our
400 knowledge. The Makran slab is bounded in the east by the Owen Fracture Zone-Dalrymple Trough
401 transform-dominated India-Arabia plate boundary that towards the north splits into the Chaman Fault
402 and Sulaiman Ranges thrust belt (Rodriguez et al., 2014). To the east, the Makran slab is bounded by
403 the Zagros collision zone where slabs have mostly detached from Arabia (Agard et al., 2011). The
404 Makran slab consists of Cretaceous ocean floor that is contiguous with the Oman ophiolites that
405 obducted onto the NE Arabian margin to the southwest (Ninkabou et al., 2021). The Makran slab
406 reaches a depth of 650 km and appears to be detached from deeper anomalies that lie directly beneath
407 in the lower mantle (Figure 5.6) which are part of the Mesopotamia slab identified by van der Meer et
408 al. (2010; 2018) and Agard et al. (2011a), interpreted to result from Mesozoic subduction below the
409 southern Eurasian margin in Iran. The Makran slab is hence representing Arabian plate lithosphere, to
410 the west of the Indian plate.

411 To the south of the Makran slab, and to the south of the India slab, the *Carlsberg slab* is located
412 at a depth of 800-1400 km (CB; Figure5), identified by Gaina et al. (2015). This is an NNE-SSW
413 trending anomaly, striking near-orthogonal to the main trend of the India slab, and in the mantle
414 reference frame, it is located below the late Cretaceous India-Arabia plate boundary. At this plate
415 boundary, a series of ophiolites were obducted that reveal evidence for west-dipping Indian lithosphere
416 subduction between ~70 and ~50 Ma, and Indian Ocean reconstructions reveal that in this time interval
417 oblique India-Arabia motion was associated with a convergent component of ~1000 km (Gaina et al.,
418 2015; Gnos et al., 1998; van Hinsbergen et al., 2019). Gaina et al. (2015) thus interpreted the Carlsberg
419 slab to have consumed oceanic lithosphere of the west Indian margin that was once located west of the
420 modern Sulaiman ranges.

421 The only slab that has so far been interpreted as Mesotethys-derived is the *Nepal slab* (NP; Figure
422 6), that is located in the depth range of 1500 – 2200 km in the lower mantle below the Himalaya. The
423 slab is NW-SE trending and south-dipping. Van Der Voo et al. (1999), van der Meer et al. (2018), and
424 Parsons et al. (2020) interpreted this anomaly as Mesotethyan, subducted during northward subduction
425 below Qiangtang during the closure of the Bangong-Nujiang Ocean until Early Cretaceous.

426 Located to the south of the India slab is the *Maldives anomaly*, a NW-SE trending slab that is
427 located beneath the north-western Indian Ocean, between ~1200 and 2200 km depth (Figure 6). This
428 slab was first identified by van der Voo et al. (1999) and was interpreted to reflect Neotethyan
429 subduction at an intra-oceanic subduction zone that had been interpreted to explain the geological record
430 of the Kohistan arc of Pakistan, as well as ophiolites of the Zagros and Himalayan orogens (Tapponnier

431 et al., 1981). This interpretation was later also adopted by van der Meer et al. (2010) and van Hinsbergen
432 et al. (2012) citing geological arguments for a Cretaceous obduction of ophiolites onto the Himalayas
433 based on sedimentological and paleomagnetic interpretations (Abrajevitch et al., 2005; Corfield et al.,
434 2005). Hafkenscheid et al. (2006) compared slab volumes with plate reconstructions and found that the
435 India and Maldives slab together correspond to a larger volume than expected from solely India-Asia
436 convergence. Assuming that all anomalies below India are Neotethyan, they explained the excess
437 volume by interpreting that the Maldives anomaly connects to the deep part of the India anomaly and
438 has a flat-lying portion from $\sim 20^{\circ}\text{S}$ to the equator that resulted from Cretaceous roll-back that would
439 have opened a back-arc basin along the south Tibetan margin, a scenario like Kapp and DeCelles (2019).
440 Closure of the back-arc basin then explains the excess volume of the combined India-Maldives slab. By
441 the time van der Meer et al. (2018) made their compilation, new sedimentological and paleomagnetic
442 data from the Himalayas and Indus-Yarlung ophiolites, as well as new explanations for the older data
443 of Abrajevitch et al. (2005) and Corfield et al. (2005) had been presented. These showed that obduction
444 of ophiolites onto the northern Indian margin occurred shortly before collision with Asia, in Eocene
445 time (Garzanti & Hu, 2015; W. Huang et al., 2015). Van der Meer et al. (2018) thus no longer interpreted
446 the Maldives slab as Neotethyan, although they offered no alternative interpretation. Parsons et al.
447 (2020) recently argued again that the Maldives slab requires a Cretaceous equatorial subduction zone,
448 but their interpretation also relied on the assumption that the Maldives slab is of Neotethyan origin. We
449 will return to the paleogeographic interpretation of the Maldives slab in the discussion section. We note
450 that the Maldives slab has been defined based on its shallowest portion: the deeper portions of the slab
451 are flat-lying and reach as far south as the equator, or beyond (Figure 6).

452 The deepest anomalies in the mantle below India and Tibet represent the *Central China slab* (CC;
453 Figure 6) which connects to an anomaly that covers much of the core-mantle boundary below the Indian
454 ocean that we here identify as the *Sri Lanka slab* (SR; Figure 6). The Central China slab is a south-
455 dipping slab that is in the lower mantle from ~ 1500 km depth to the base of the mantle. It was originally
456 included in the Mongol-Kazakh slab (van der Meer et al., 2018), interpreted as the relics of the Mongol-
457 Okhotsk ocean (Van Der Voo et al., 1999) that intervened North China and Siberia until the latest
458 Jurassic (Van Der Voo et al., 2015), but it was later interpreted as a separate anomaly by van der Meer
459 et al. (2018), who considered it possible that the slab is related to the latest Triassic closure of the
460 Paleotethys ocean between the Qiangtang and NE Tibetan terranes. The Sri Lanka slab is found
461 horizontally draping the core-mantle boundary below the Indian ocean and continent and Tibet (Figure
462 6,8).

463

464 4. Discussion

465 4.1 Paleotethyan and Mesotethyan slabs below India and Tibet

466 To analyse the plate kinematic context of slab detachment during ongoing trench and plate
467 motion, we aim to identify the slabs that unequivocally detached from the Indian plate, and whose
468 geological records are hence located in the Himalayas or southern Tibet. Previous tomographic
469 analyses all assumed that each slab located below India and Tibet to the south of the Indus-Yarlung
470 suture reflect Neotethyan lithosphere and we therefore first assess where remains of the Triassic-Early
471 Cretaceous Mesotethyan subduction and Permo-Triassic Paleotethyan subduction may reside.

472 Geological evidence shows that subduction during Paleotethys and Mesotethys closure
473 occurred both northward, below blocks that already accreted to the Tibetan margin, at mantle-
474 stationary trenches, as well as southward and retreating during the northward motion of the migrating
475 Qiangtang (during Paleotethys closure) and Lhasa terranes (during Mesotethys closure). Hence, in
476 both instances, slab walls may have formed below the northern, Tibetan margin, and flat-lying slabs
477 covering a few thousand km to the south of these walls.

478 The Sri Lanka slab overlying the core-mantle boundary is a clear candidate to represent the
479 Paleotethys lithosphere that was consumed by southward subduction below the Qiangtang terrane
480 during its northward flight to Eurasia. The Sri Lanka slab connects to the steeply dipping Central
481 China slab that could represent the last parts of the southward subducted Paleotethyan lithosphere
482 which have not reached the core-mantle boundary yet. Additionally, northward subducted
483 Paleotethyan lithosphere could be contained in the ‘slab graveyard’ at the core-mantle boundary to the
484 north of the Central China slab. Alternatively, the Central China anomaly may contain both north- and
485 southward subducted lithosphere. The global correlations of slabs and geological records of van der
486 Meer et al. (2018) suggests that slab walls, subducted at stable trenches, tend to sink into the lower
487 mantle without the delay that flat-lying slabs, which subducted at migrating trenches, experience. But
488 if subduction of the Paleotethys oceanic lithosphere was indeed double-sided, the final collision
489 would have been a soft docking, since no slab pulls one continent below the other, and an upright
490 folded lithosphere like the Molucca Sea slabs today (Hall & Spakman, 2015) would ‘detach’ from the
491 surface. We speculate that such vertically arched ‘slab folds’ may sink slower than a single detached
492 slab as sub-slab mantle under the slab-arch geometry needs to be removed sideways which could
493 explain the still upright portion of the Central China slab.

494 The only slab that has thus far been interpreted as Mesotethys-derived is the Nepal slab (Figure
495 5,6). This slab is less than 1000 km in vertical extent, and appears much less thickened than e.g., the
496 India slab. Because the width of the Mesotethys Ocean was like the Paleo- and Neotethys, it is
497 unlikely that the Nepal slab contains all Mesotethys lithosphere. The evidence for Triassic to early
498 Cretaceous subduction below the Lhasa terrane, e.g. in the form of arc magmatic rocks (Kapp &

499 Decelles, 2019; S. Li et al., 2019), moreover, suggests that there was subduction of lithosphere below
500 the Lhasa terrane throughout its northward flight towards Eurasia. Kapp & Decelles (2019) suggested
501 this was Neothethyan lithosphere subducting northward since the Triassic. We consider this unlikely:
502 paleomagnetic data place Lhasa against the northern Gondwana margin in the late Triassic (Li et al.,
503 2016), followed by Neotethys opening until the early Cretaceous. In this view, a south-directed
504 subduction zone as suggested by Zhu et al. (2015), would be more likely. Either way, a flat-lying slab
505 is expected of similar magnitude as that of the Paleotethys (overturned if subducted northward,
506 normal facing if subducted southward) at a shallower position in the mantle. We infer that the Nepal
507 slab is the northern tip of a flat-lying slab that continues southward until near-equatorial latitudes and
508 includes (at least part of) the Maldives slab (Figure 5,6). This interpretation assigns a similar
509 dimension to the Mesotethys and Paleotethys-derived slabs as dictated by plate tectonic
510 reconstructions. Below the massive slab wall of the India slab, this horizontal slab Nepal-Maldives
511 slab would then be bent down under the likely faster sinking India slab wall (Figure8). The Nepal slab
512 may then represent the remnants of an arched slab 'fold'.

513 Realizing that a large part of the mid-mantle anomalies below India may be Mesotethyan
514 lithosphere rather than Neotethyan makes interpreting the Maldives slab as Neotethys not a necessity.
515 As outlined above, there is no conclusive geological evidence that a slab detached at an equatorial
516 intra-oceanic subduction zone upon arrival of the northern Indian margin in the trench. Parsons et al.
517 (2020) recently concluded that the Maldives slab is the conclusive evidence to this end, but this
518 argument relied on the assumption that all sub-Indian plate anomalies are Neotethyan. Tomographic
519 evidence does not exclude an equatorial subduction zone, since the shallower part of the Maldives
520 slab could be a separate anomaly that lies on top of a flat-lying Mesotethys slab. However, an intra-
521 oceanic equatorial subduction zone is not required by the tomographic model. Below, we focus our
522 analysis on the anomalies whose Neotethyan affinity is undisputed. This includes the India, Himalaya,
523 Carlsberg, Hindu Kush, Burma, and Chaman slabs and the horizontally underthrust Indian lithosphere
524 below Tibet.

525

526 4.2 Timing of Neotethyan slab detachment events

527 Of the youngest slabs that consumed Indian plate lithosphere, the Chaman and Burma slabs are
528 still connected to the Indian plate, the Hindu Kush slab is in the process of breaking off (Kufner et al.,
529 2021), and the Himalaya, Carlsberg, and India slabs are detached. We first evaluate when this
530 detachment occurred, then evaluate the kinematic setting in which detachment occurred, and finally
531 briefly evaluate the potential to detect geological signatures of this detachment from Himalayan
532 geology.

533 We estimate of the timing of detachment of the Himalayas through kinematic restoration of
534 the timing and duration of horizontal Indian underthrusting below Tibet. Kinematic reconstructions of
535 India-Asia convergence combined with reconstruction of Tibetan shortening (van Hinsbergen et al.,
536 2019) shows that the modern northern margin of the underthrust Indian plate lithosphere imaged by
537 seismological data (Agius & Lebedev, 2013; Chen et al., 2017; van Hinsbergen et al., 2019)
538 underthrusts below the Himalayas thrust front around 30-25 Ma at the syntaxes, becoming
539 progressively younger towards the central-eastern Himalayas to around 15-13 Ma. This suggests that
540 the Himalayas slab detached diachronously, starting around 25 Ma at the western and eastern syntaxes
541 and progressively migrating inwards towards the central-eastern part of the plate boundary around 15
542 Ma (van Hinsbergen et al., 2019). Or, alternatively, detachment may have occurred at a deeper level,
543 after which the remaining Indian lithosphere rebounded back to a horizontal position (Magni et al.,
544 2017), although with the continued northward advance below Tibet, an inclined Indian margin would
545 have acted as a plow (Hinsbergen et al., 2020) which could have prevented such a rebound. When
546 viewed in a mantle frame of reference (Dobrovine et al., 2012), the reconstruction of van Hinsbergen
547 et al. (2019) places the Himalayas thrust front above the modern position of the Himalayas slab. We
548 therefore favour an interpretation that detachment of the Himalayas slab coincided with the base of
549 the continental Indian lithosphere and that this lithosphere horizontally underthrusts Tibet.

550 The Hindu Kush slab in the west must represent a lateral equivalent of the Himalayas slab
551 that escaped Miocene detachment, or, more likely, where detachment occurred at a deeper level. The
552 Hindu Kush slab is ~600 km long and is offset southward from the northernmost part of the
553 underthrust Indian lithosphere below the Pamir by ~300 km (Figure 5). Hence, when detachment of
554 the Himalayas slab from the westernmost Indian lithosphere now below the Pamir crust occurred
555 around 25 Ma, about 300 km of the Hindu Kush slab was likely still located at the surface adjacent to
556 India's northwestern margin, but the remaining deepest 300 km of the Hindu Kush lithosphere had
557 already subducted then. The volume of the Himalayas slab suggests it contains more than 300 km of
558 subducted lithosphere and is thus not a detached equivalent of the Hindu Kush slab: detachment of the
559 Himalayas slab more likely removed a deeper part of the Hindu Kush slab and detached at a greater
560 depth, of up to some 300 km, than at the north Indian continental margin where it detached at the
561 depth of the base of the lithosphere.

562 Estimating the timing of decoupling between the Himalayas and India slabs is more
563 challenging. The Himalayas slab is ~500 km long and depending on the assumed amount of
564 thickening may contain two or three times that length in lithosphere. Comparing this with estimates of
565 India-Asia convergence suggests that the Himalayas slab contains lithosphere that subducted
566 sometime between ~40-35 Ma and 25-15 Ma (Replumaz et al., 2010). Hence, if detachment occurred
567 at shallow depth, it would have occurred around 40-35 Ma. However, if detachment occurred at

568 greater depth, e.g. around 300 km as argued above for the Hindu Kush slab, detachment occurred
569 later, after at least part of the Himalayas slab had already been subducted.

570 The Carlsberg slab in the west was interpreted to contain lithosphere that subducted during highly
571 oblique convergence between India and Arabia, between the Maastrichtian onset of subduction recorded
572 by ophiolites in the Sulaiman ranges (Gaina et al., 2015; Gnos et al., 1998). Upper Paleocene to lower
573 Eocene clastics in the Sulaiman ranges with ophiolite detritus (Khan & Clyde, 2013) show that
574 obduction was underway by 60-55 Ma, and arrest of convergence and final emplacement was estimated
575 at ~50 Ma (Gaina et al., 2015; Gnos et al., 1998). When placed in a mantle frame of reference
576 (Dobrovine et al., 2012), the west Indian margin at 50 Ma is located above the Carlsberg slab.
577 Moreover, reconstructions of India-Arabia motion using Indian ocean basin reconstructions (DeMets
578 & Merkouriev, 2021; Gaina et al., 2015) reveal that post-50 Ma India-Helmand convergence at the
579 latitude of the Chaman slab was associated with an E-W component of convergence of ~500-600 km
580 (alongside a much larger component of left-lateral strike-slip motion) coincident with the Chaman slab
581 length. A 50 Ma detachment age of the Carlsberg slab thus seems a reasonable estimate.

582

583 4.3 Slab detachment during ongoing convergence: concept and future study areas

584 The plate kinematic history during which modern mantle structure evolved, reveals that despite
585 ongoing plate convergence and absolute northward motion of the Indian plate and the plate boundary
586 along southern Tibet, multiple slab detachment events occurred. An important corollary of this history
587 is that commonly assumed geodynamic conditions used to simulate slab detachment in numerical and
588 analogue experiments – an arrest of plate convergence, and a mantle-stationary trench – did not apply
589 when the slabs detached from subducting Indian plate lithosphere. Two first-order differences between
590 model predictions and the reconstructed history of slab detachments from the Indian plate follow
591 straightforwardly from our analysis above.

592 First, the ongoing plate convergence between India and Asia implies that there cannot have
593 been a long delay time between subduction and detachment of a slab. Model predictions suggest that
594 slabs break-off 5-30 Ma after their subduction following a phase of gradual shearing and viscous
595 necking (Andrews & Billen, 2009; Bercovici & Skemer, 2017; Duretz et al., 2012; Gerya et al., 2004;
596 Royden, 1993). Plate convergence rates in the last 45 Ma have varied from 4-8 cm/a (DeMets &
597 Merkouriev, 2021) of which no more than ~2 cm/a was accommodated by upper plate shortening in
598 Tibet (van Hinsbergen et al., 2019). Hence, for every 1 Ma delay time between subduction and
599 detachment, a potential necking zone in a slab would sink 20-60 km. After the last phase of slab
600 detachment from the northern Indian margin, no detectable slab has formed and the horizontal offset
601 between the north Indian margin imaged below Tibet and the Himalayas slab shows that detachment

602 must have occurred quickly (within a few Ma) after arrival of that margin at the trench, and at a shallow
603 depth around the base of the lithosphere.

604 Second, detachment was probably not only caused by vertical stretching of lithosphere. The
605 Carlsberg slab was subducting westwards while India moved northwards: it is inevitable that this slab
606 was dragged sideways through the mantle during its subduction, and during the arrival of the Indian
607 continental lithosphere in the trench. At present, lateral slab dragging occurs with the Chaman and
608 Burma slabs (Figure 7), and has also been shown for the Tonga-Kermadec and Gibraltar slabs (van de
609 Lagemaat et al., 2018; Spakman et al., 2018; Parsons et al., 2021). This dragging of the Carlsberg slab
610 must have been resisted by the ambient mantle leading to a slab-strike parallel resistive shear traction
611 (Spakman et al. 2018) that may have aided break-off as this viscous coupling between slab and mantle
612 may cause large slab-strike parallel deformation (Giardini and Woodhouse 1986; Chertova et al. 2018).
613 Such northward dragging not only applies to the slabs on the west and east side of India, but also follows
614 from our analysis of the Hindu Kush slab. The slab is currently located ~300 km to the south of the
615 northern edge of the Indian plate located below the Pamir (Figure 5), and this may reflect that the slab
616 retreated relative to India over this distance since the detachment of the Himalayas slab from India's
617 northwestern margin some 25-30 Ma ago (cf. the 3D convergence-detachment model of Duretz et al.
618 2014). But in that same time period, the Indian plate moved >1000 km northward. The Hindu Kush slab
619 must thus have been dragged northward over some 700 km through the mantle in the last ~25 Ma,
620 consistent with its offset relative to the Himalayas slab. Such a history of northward advance also
621 applies to the Himalayas slab given its overturned orientation. Hence, the ongoing absolute motion of
622 the Indian plate adds an oppositely directed force on the slab as mantle material must be removed in
623 front of the slab to accommodate forward slab transport. This forcing may localize where the slab is
624 weakest which is classically the slab bending zone below the trench but may also occur deeper due to
625 subducted lithosphere weakness (Gerya et al., 2021). In this scenario, the slab can be sheared-off
626 shallowly, i.e., near the base of the lithosphere of the downgoing plate (Figure 9) which contrasts with
627 the lithosphere-age dependent detachment depth inferred from previous modelling.

628 The question then arises whether slab detachment during ongoing plate motion and trench
629 advance yields geological signatures that are like the vertical necking that is portrayed in classical
630 experiments. The detailed earthquake hypocenter studies in the Hindu Kush slab of Kufner et al. (2017;
631 2021) elegantly show that the shear zone along which detachment is occurring mimics the predicted
632 shear zones by vertical necking experiments (Duretz et al., 2011), even though the Hindu Kush slab is
633 being dragged northward. On the other hand, with ongoing absolute plate motion of the downgoing
634 plate, a detachment zone is immediately being overridden. The classically suggested high-temperature
635 pulse that was inferred to cause magmatism or metamorphism in a suture zone (van de Zedde and
636 Wortel, 2001), may therefore not be recorded in the collision zone.

637 To determine the geological effects of slab detachment during ongoing plate and trench
638 migration and to evaluate whether there is dependence of geological signatures on the absolute plate
639 motion direction relative to slab strike, calls for future numerical and analogue experiments in
640 combination with field testing. To determine the effects of near slab-strike parallel dragging, we identify
641 the Chaman and Burma slabs as key candidates for the study of present-day geophysical expressions.
642 Effects on the longer geological evolution associated with detachment associated with slab-strike
643 parallel dragging may be contained in the Eocene geological record of the Sulaiman Ranges of Pakistan.

644 The highly detailed studies of Kufner et al. (2016; 2017; 2021) of the Hindu Kush slab provide
645 key constraints for detachment during slab-strike perpendicular dragging. The Miocene geological
646 record of the Himalayas would provide a longer-term geological perspective on the effects of slab
647 detachment during plate motion. In that light, the study of Webb et al. (2017) is intriguing: Those
648 authors interpreted an evolution of slab detachment below the Himalayas that started in the syntaxes
649 around 30-25 Ma and progressed to the central-eastern Himalayas until ~13 Ma. They concluded an
650 identical timing and asymmetry in detachment age as we infer from the shape of the horizontally
651 underthrust northern Indian margin below Tibet (Figure 5,6,7), but based this on an entirely independent
652 data set and line of argumentation. Their study was based on along-strike studies of the Himalayas and
653 southern Tibet and identified trends in high-K and adakitic magmatism and geochronological estimates
654 of major ductile faults in the orogen. The study of Webb et al. (2017), but also earlier studies arguing
655 for a ~25 Ma onset for changing thermal conditions in the collision zone (Maheo et al., 2002), may thus
656 provide an excellent starting point for hypothesis building as basis for numerical and analogue
657 experiments of slab detachment during ongoing plate convergence and trench motion.

658 Also, the recent unprecedented high-resolution India-Asia convergence records of DeMets and
659 Merkouriev (2021) provide key information. During the inferred detachment period between ~30-25
660 and 13 Ma they showed a subtle slow-down in plate convergence rates and following 13 Ma a steady
661 rate of ~4 cm/a. Intriguingly, India-Asia convergence accelerated by a few cm/a between 40 and 30 Ma,
662 around which time the detachment of the Himalayas slab from the India slab may have occurred. This
663 detachment would have potentially removed the mantle resistance against northward slab dragging
664 removing, at least temporarily, this control on the northward motion of the Indian plate, but also this
665 speculation requires future dynamic analysis.

666 Finally, we note that the initial India-Asia collision recorded in the Tibetan Himalayas around
667 60-50 Ma (An et al., 2021; Najman et al., 2010) is widely interpreted to be followed by slab detachment
668 along the Indian continental margin under the assumption that this collision represented the arrival of
669 the contiguous Indian continent at the Tibetan trench (Kohn et al., 2002; H. Lee et al., 2009; Zhu et al.,
670 2015). If there was slab detachment in the late Paleocene or early Eocene, it is not detectable within the
671 India anomaly. We note that Indian plate subduction rates in this time period were in excess of 150

672 km/Ma (DeMets & Merkouriev, 2021; van Hinsbergen et al., 2019): even if slab detachment occurred
673 in this time period, it could have taken only a few Ma for a slab to reach to the base of the upper mantle
674 again and it is questionable whether there would have been any detectable dynamic or geological
675 response. The kinematic restoration of van Hinsbergen et al. (2012; 2019) interpreted the Paleocene-
676 early Eocene collision reconstructed from the northern Himalayas as recording the arrival of a
677 microcontinent at the southern Eurasian margin and interpreted the modern northern margin of India
678 underthrust below Tibet as the former passive margin of northern India that only arrived at the
679 southern Himalayan margin in the Miocene. Subduction of microcontinental lithosphere without slab
680 detachment is common in Tethyan mountain belts (van Hinsbergen and Schouten, 2021) and this
681 scenario would suggest that detachment of the Himalayas slab occurred along the passive continental
682 margin, as commonly inferred in slab detachment models. If all lithosphere that subducted in the
683 Himalayas after the early Eocene (Hu et al., 2016; Ingalls et al., 2016; Replumaz et al., 2010) or late
684 Eocene (Aitchison et al., 2007; Jagoutz et al., 2015; Martin et al., 2020) was continental, as more
685 commonly assumed, the timing, causes, and locations of slab break-off within continental lithosphere
686 following 1000 km or more of rapid continental subduction, remain to be explained.

687

688 5. Conclusions

689 Slab detachment is a key process in the plate tectonic cycle and may have profound impact on the
690 geological record of orogens causing metamorphism, magmatism, economic mineralization, and
691 surface uplift, and may be associated with plate reorganizations. Conceptual, numerical, and analogue
692 models that aim to find the dynamic link between slab detachment and these geological observations
693 assume that plate convergence stops prior to detachment, that the slab and trench remain mantle-
694 stationary for 10 Ma or more, and that slab detachment is then a gradual and laterally diachronous
695 process. However, plate convergence typically continues, and trenches are rarely mantle-stationary
696 during slab detachment. In this paper, we investigate the history of slab detachments from the Indian
697 plate to develop a kinematic framework for slab detachment during ongoing absolute plate and trench
698 motion. Seismic tomography has long shown that no major slabs are currently attached to the Indian
699 plate below the Himalaya, and major anomalies located in the upper and lower mantle below India
700 have widely been interpreted as detached relict slabs. All these slabs are located far south of the
701 modern northern margin of the Indian continent that is seismically imaged to horizontally underthrust
702 the Tibetan Plateau. The offset between the slabs and the margin from which they detached is
703 consistent with the kinematic evidence that India's absolute plate motion continued throughout the
704 Cenozoic until the present day.

705 To identify which slabs must have broken off the fast-moving Indian plate, we first update the
706 correlation of subducted slabs below India and Tibet to lithosphere that subducted in Mesozoic-

707 Cenozoic time. The slabs below India were among the first identified following the advent of global
708 tomography and were initially all assumed to represent Neotethyan lithosphere. Because their volume
709 far exceeds volumes predicted from India-Asia convergence reconstructions, intra-oceanic subduction
710 was inferred within the Neotethyan realm. But global correlations have shown that slabs that
711 subducted in Permo-Triassic and Jurassic time are generally also still imaged in the lower mantle. In
712 the case of the mantle beneath the Indian plate, slabs that comprise of the Mesotethys that subducted
713 in Late Triassic-Early Cretaceous time and Paleotethys (Permian - Late Triassic) oceanic lithosphere
714 should still be visible. We use first-order estimates of expected slab shape and length to infer that a
715 Paleotethyan derived slab (here named Sri Lanka slab) is located at the base of the mantle and may
716 include part of the previously identified Central China slab below northern Tibet. A Mesotethyan slab
717 horizontally underlies the India slab wall in the mid-mantle and includes the previously identified
718 Maldives and Nepal anomalies. Whereas tomography does not exclude that an equatorial Neotethyan
719 slab may have formed, such an interpretation is not required to explain the tomography. Only of the
720 India, Carlsberg, and Himalayas slabs we are confident that they must represent Neotethyan
721 lithosphere that detached from the Indian plate. The India and Himalayas slabs detached from the
722 northern plate margin, the Carlsberg slab from the western margin. In addition, the Hindu Kush,
723 Burma, and the newly identified Chaman slabs are still attached to India.

724 We identify that the three detached Neotethyan slabs (India, Carlsberg, Himalayas slabs)
725 detached during ongoing northward motion of India relative to the mantle. During their detachment,
726 they were not passively dangling in the mantle during which time gradual necking would lead to
727 detachment, but we hypothesize that in addition to slab pull the resistance of the mantle against
728 forward slab dragging of laterally wide slabs may have played a key role. We discuss that slab
729 detachment during ongoing plate motion may have different geological expressions than inferred from
730 previous detachment modelling, and that these may differ as function of slab strike relative to absolute
731 plate motion direction. Slabs to the west (Chaman) and east (Burma) of India are dragged near slab-
732 strike parallel through the mantle, and detachment under those circumstances must have affected the
733 older, deeper, Carlsberg slab as well. The latter slab likely detached in Eocene time, and we identify
734 the Sulaiman Ranges of west Pakistan as key area to test possible signatures (Figure 10).

735 Slabs at the northern extent of the Indian plate detached following and during slab advance.
736 This is illustrated by the northward overturned Himalayas slab that was the last to detach. An entirely
737 independent, previously published estimate of the last phase of slab detachment using magmatism and
738 exhumation patterns in the Himalayas coincides with our estimate of the last phase of detachment on
739 kinematic restoration of horizontally underthrust northern Indian margin below Tibet and may provide
740 a geological record to calibrate the geological effects of detachment during ongoing downward plate
741 motion. In addition, the well-documented active detachment in the Hindu Kush slab, which we show
742 was dragged through the mantle over a distance close to 700 km in the Cenozoic, may provide a

743 geophysical record of detachment of a forwardly dragged slab. Our analysis thus provides new
744 conditions for slab detachment to occur in the geodynamic context of ongoing relative and absolute
745 plate motions, which may be used by numerical and analogue experiments to evaluate geological
746 signatures of this key geodynamic process.

747

748

749 Acknowledgements

750 AQ, NL, and DJJvH acknowledge funding through Netherlands Organization for Scientific
751 Research (NWO) Vici grant 865.17.001 to DJJvH.

752

753 References

754 Abrajevitch, A. V, Ali, J. R., Aitchison, J. C., Davis, A. M., Liu, J., & Ziabrev, S. V. (2005).
755 Neotethys and the India – Asia collision : Insights from a palaeomagnetic study of the Dazhuqu
756 ophiolite , southern Tibet, 233, 87–102. <https://doi.org/10.1016/j.epsl.2005.02.003>

757 Agard, P., Omrani, J., Jolivet, L., Whitechurch, H., Vrielynck, B., Spakman, W., et al. (2011a).
758 Zagros orogeny: A subduction-dominated process. *Geological Magazine*, 148(5–6), 692–725.
759 <https://doi.org/10.1017/S001675681100046X>

760 Agard, P., Omrani, J., Jolivet, L., Whitechurch, H., Vrielynck, B., Spakman, W., et al. (2011b).
761 Zagros orogeny: A subduction-dominated process. *Geological Magazine*, 148(5–6), 692–725.
762 <https://doi.org/10.1017/S001675681100046X>

763 Agius, M. R., & Lebedev, S. (2013). Tibetan and Indian lithospheres in the upper mantle beneath
764 Tibet: Evidence from broadband surface-wave dispersion. *Geochemistry, Geophysics,*
765 *Geosystems*, 14(10), 4260–4281. <https://doi.org/10.1002/ggge.20274>

766 Aitchison, J. C., Ali, J. R., & Davis, A. M. (2007). When and where did India and Asia collide ?
767 *Journal of Geophysical Research*, 112(November 2006), 1–19.
768 <https://doi.org/10.1029/2006JB004706>

769 Amaru, M. (2007). *Global travel time tomography with 3-D reference models. Geologica Ultraiectina*
770 (Vol. 274).

771 Andrews, E. R., & Billen, M. I. (2009). Rheologic controls on the dynamics of slab detachment.
772 *Tectonophysics*, 464(1–4), 60–69. <https://doi.org/10.1016/j.tecto.2007.09.004>

- 773 Atherton, M. P., & Ghani, A. A. (2002). Slab breakoff: a model for Caledonian, Late Granite syn-
774 collisional magmatism in the orthotectonic (metamorphic) zone of Scotland and Donegal,
775 Ireland. *LITHOS*, 62, 65–85.
- 776 Běhounková, M., & Čížková, H. (2008). Long-wavelength character of subducted slabs in the lower
777 mantle. *Earth and Planetary Science Letters*, 275, 43–53.
778 <https://doi.org/10.1016/j.epsl.2008.07.059>
- 779 Bercovici, D., & Skemer, P. (2017). Grain damage, phase mixing and plate-boundary formation.
780 *Journal of Geodynamics*, 108(April), 40–55. <https://doi.org/10.1016/j.jog.2017.05.002>
- 781 Bercovici, D., Schubert, G., & Ricard, Y. (2015). Abrupt tectonics and rapid slab detachment with
782 grain damage. *PNAS*, 112(5). <https://doi.org/10.1073/pnas.1415473112>
- 783 Bijwaard, H., Spakman, W., & Engdahl, E. R. (1998). Closing the gap between regional and global
784 travel time tomography. *Journal of Geophysical Research: Solid Earth*, 103(B12), 30055–
785 30078. <https://doi.org/10.1029/98jb02467>
- 786 Billen, M. I. (2010). Slab dynamics in the transition zone. *Physics of the Earth and Planetary
787 Interiors*, 183, 296–308. <https://doi.org/10.1016/j.pepi.2010.05.005>
- 788 Boschman, L. M., van Hinsbergen, D. J. J., Kimbrough, D. L., Langereis, C. G., & Spakman, W.
789 (2018). The Dynamic History of 220 Million Years of Subduction Below Mexico: A Correlation
790 Between Slab Geometry and Overriding Plate Deformation Based on Geology, Paleomagnetism,
791 and Seismic Tomography. *Geochemistry, Geophysics, Geosystems*, 19(12), 4649–4672.
792 <https://doi.org/10.1029/2018GC007739>
- 793 Buitter, S. J. H., & Pfiffner, O. A. (2003). Numerical models of the inversion of half-graben basins,
794 22(5), 1–16. <https://doi.org/10.1029/2002TC001417>
- 795 Buitter, S. J. H., Govers, R., & Wortel, M. J. R. (2002). Two-dimensional simulations of surface
796 deformation caused by slab detachment, 354, 195–210.
- 797 Burke, K., Steinberger, B., Torsvik, T. H., & Smethurst, M. A. (2008). Plume Generation Zones at the
798 margins of Large Low Shear Velocity Provinces on the core – mantle boundary, 265, 49–60.
799 <https://doi.org/10.1016/j.epsl.2007.09.042>
- 800 Butterworth, N. P., Talsma, A. S., Müller, R. D., Seton, M., Bunge, H. P., Schuberth, B. S. A., et al.
801 (2014). Geological, tomographic, kinematic and geodynamic constraints on the dynamics of
802 sinking slabs. *Journal of Geodynamics*, 73, 1–13. <https://doi.org/10.1016/j.jog.2013.10.006>
- 803 Byrne, D. E., Sykes, L. R., & Davis, D. A. N. M. (1992). Great Thrust Earthquakes and Aseismic Slip
804 Along the Plate Boundary of the Makran motion in the form of earthquakes may occur in a

805 variety (e . g ., southern Chile), while still others have experienced no of ways at subduction
806 zones . Some margins produ. *Journal of Geop*, 97(91), 449–478.

807 Chemenda, A. I., Mattauer, M., Malavieille, J., & Bokun, A. N. (1995). normal faulting : Results from
808 physical modelling. *Earth and Planetary Science Letters*, 132, 225–232.

809 Chen, M., Niu, F., Tromp, J., Lenardic, A., Lee, C. A., Cao, W., & Ribeiro, J. (2017). Lithospheric
810 foundering and underthrusting imaged beneath Tibet. *Nature Communications*, 8, 1–10.
811 <https://doi.org/10.1038/ncomms15659>

812 Conrad, C. P., & Lithgow-Bertelloni, C. (2002). How mantle slabs drive plate tectonics. *Science*,
813 298(5591), 207–209. <https://doi.org/10.1126/science.1074161>

814 Copley, A., Avouac, J. P., & Royer, J. Y. (2010). India-Asia collision and the Cenozoic slowdown of
815 the Indian plate: Implications for the forces driving plate motions. *Journal of Geophysical*
816 *Research: Solid Earth*, 115(3), 1–14. <https://doi.org/10.1029/2009JB006634>

817 Corfield, R. ., Watts, A. ., & Searle, M. . (2005). Subsidence history of the north Indian continental
818 margin , Zaskar – Ladakh. *Journal Ofthe Geological Society, London*, 162(1991), 135–146.

819 Le Dain, Y. A., Topponnier, P., & Molnar, P. (1984). Active Faulting And Tectonics Of Burma And
820 Surrounding Regions. *Journal of Geophysical Research*, 89(Figure 1), 453–472.

821 Davies, J. H., & von Blanckenburg, F. (1995). Slab breakoff: A model of lithosphere detachment and
822 its test in the magmatism and deformation of collisional orogens. *Earth and Planetary Science*
823 *Letters*, 129(1–4), 85–102. [https://doi.org/10.1016/0012-821X\(94\)00237-S](https://doi.org/10.1016/0012-821X(94)00237-S)

824 DeMets, C., & Merkouriev, S. (2021). Detailed reconstructions of India-Somalia plate motion, 60 Ma
825 to present: Implications for Somalia plate absolute motion and India-Eurasia plate motion.
826 *Geophysical Journal International*, 1730–1767. <https://doi.org/10.1093/gji/ggab295>

827 Domeier, M., Doubrovine, P. V., Torsvik, T. H., Spakman, W., & Bull, A. L. (2016). Global
828 correlation of lower mantle structure and past subduction. *Geophysical Research Letters*, 43(10),
829 4945–4953. <https://doi.org/10.1002/2016GL068827>

830 Doubrovine, P. V, Steinberger, B., & Torsvik, T. H. (2012). Absolute plate motions in a reference
831 frame defined by moving hot spots in the Pacific , Atlantic , and Indian oceans. *Journal of*
832 *Geophysical Research*, 117(July), 1–30. <https://doi.org/10.1029/2011JB009072>

833 Duretz, Gerya, T. V., & May, D. A. (2011). Numerical modelling of spontaneous slab breakoff and
834 subsequent topographic response. *Tectonophysics*, 502(1–2), 244–256.
835 <https://doi.org/10.1016/j.tecto.2010.05.024>

836 Duretz, T., Schmalholz, S. M., & Gerya, T. V. (2012). Dynamics of slab detachment. *Geochemistry*

- 837 *Geophysics Geosystems*, 13(3). <https://doi.org/10.1029/2011GC004024>
- 838 Duret, T., Gerya, T. V., & Spakman, W. (2014). Slab detachment in laterally varying subduction
839 zones: 3-D numerical modeling. *Geophysical Research Letters*, 41(6), 1951–1956.
840 <https://doi.org/10.1002/2014GL059472>
- 841 Ely, K. S., & Sandiford, M. (2010). Seismic response to slab rupture and variation in lithospheric
842 structure beneath the Savu Sea, Indonesia. *Tectonophysics*, 483(1–2), 112–124.
843 <https://doi.org/10.1016/j.tecto.2009.08.027>
- 844 Fernández-garcía, C., Guillaume, B., & Brun, J. (2019). Tectonophysics 3D slab break off in
845 laboratory experiments. *Tectonophysics*, 773(October), 1–11.
846 <https://doi.org/10.1016/j.tecto.2019.228223>
- 847 Forsyth, D., & Uyedat, S. (1975). On the Relative Importance of the Driving Forces of Plate Motion.
848 *Geophysical Journal of the Royal Astronomical Society*, 43(1), 163–200.
849 <https://doi.org/10.1111/j.1365-246X.1975.tb00631.x>
- 850 Fukao, Y., Obayashi, M., Inoue, H., & Nenbai, M. (1992). Subducting Slabs Stagnant in the Mantle
851 Transition Zone. *Journal of Geophysical Research*, 97, 4809–4822.
- 852 Fukao, Y., Widiyantoro, S., & Obayashi, M. (2001). Stagnant slabs in the upper and lower mantle
853 transition region, (1999), 291–323.
- 854 Gaina, C., Douwe, J. . van H., & Spakman, W. (2015). Tectonic interactions between India and
855 Arabia since the Jurassic reconstructed from marine geophysics, ophiolite geology, and seismic
856 tomography. *Tectonics*, 34, 875–906. <https://doi.org/10.1002/2014TC003780>.Received
- 857 Garzanti, E., & Hu, X. (2015). Latest Cretaceous Himalayan tectonics : Obduction , collision or
858 Deccan-related uplift ? *Gondwana Research*, 28(1), 165–178.
859 <https://doi.org/10.1016/j.gr.2014.03.010>
- 860 Garzanti, E., Rade, G., & Malusà, M. G. (2018). Earth-Science Reviews Slab breakoff : A critical
861 appraisal of a geological theory as applied in space and time. *Earth Science Reviews*, 177(July
862 2017), 303–319. <https://doi.org/10.1016/j.earscirev.2017.11.012>
- 863 Gerya, T V, Bercovici, D., & Becker, T. W. (2021). Dynamic slab segmentation due to brittle –
864 ductile damage in the outer rise. *Nature*, 599(November). <https://doi.org/10.1038/s41586-021-03937-x>
865
- 866 Gerya, Taras V., Yuen, D. A., & Maresch, W. V. (2004). Thermomechanical modelling of slab
867 detachment. *Earth and Planetary Science Letters*, 226(1–2), 101–116.
868 <https://doi.org/10.1016/j.epsl.2004.07.022>

- 869 Gnos, E., Khan, M., Mahmood, K., Khan, A. S., Shafique, N. A., & Villa, I. M. (1998). Bela oceanic
870 lithosphere assemblage and its relation to the \hat{A} union hotspot Re. *Tectonophysics*.
- 871 González, J. R., & Negredo, A. M. (2012). The role of the overriding plate thermal state on slab dip
872 variability and on the occurrence of flat subduction. *Geochemistry, Geophysics, Geosystems*,
873 *13*(1), 1–21. <https://doi.org/10.1029/2011GC003859>
- 874 Grand, S. P., van der hilst, R. ., & Widiyantoro, S. (1997). Global Seismic Tomography: A Snapshot
875 of Convection in the Earth. *GSA Today*, *7*(4), 1–7.
- 876 Hafkenscheid, E., Wortel, M. J. R., & Spakman, W. (2006). Subduction history of the Tethyan region
877 derived from seismic tomography and tectonic reconstructions. *Journal of Geophysical*
878 *Research: Solid Earth*, *111*(8), 1–26. <https://doi.org/10.1029/2005JB003791>
- 879 Hall, R., & Spakman, W. (2002). Subducted slabs beneath the eastern Indonesia-Tonga region:
880 Insights from tomography. *Earth and Planetary Science Letters*, *201*(2), 321–336.
881 [https://doi.org/10.1016/S0012-821X\(02\)00705-7](https://doi.org/10.1016/S0012-821X(02)00705-7)
- 882 Hall, R., & Spakman, W. (2015). Tectonophysics Mantle structure and tectonic history of SE Asia.
883 *Tectonophysics*, *658*, 14–45. <https://doi.org/10.1016/j.tecto.2015.07.003>
- 884 Hébert, R., Bezar, R., Guilmette, C., Dostal, J., Wang, C. S., & Liu, Z. F. (2012). The Indus –
885 Yarlung Zangbo ophiolites from Nanga Parbat to Namche Barwa syntaxes , southern Tibet :
886 First synthesis of petrology , geochemistry , and geochronology with incidences on geodynamic
887 reconstructions of Neo-Tethys. *Gondwana Research*, *22*(2), 377–397.
888 <https://doi.org/10.1016/j.gr.2011.10.013>
- 889 Hilst, R. D. Van Der, Engdahl, R., Spakman, W., & Nolet, G. (1991). Tomographic imaging of
890 subducted lithosphere below northwest Pacific island arcs. *Nature*, *353*.
- 891 Hilst, R. D. Van Der, Widiyantoro, S., & Engdahl, E. R. (1997). Evidence for deep mantle circulation
892 from global tomography. *Nature*, *386*(April).
- 893 van Hinsbergen, D. J. J., Hafkenscheid, E., Spakman, W., Meulenkamp, J. ., & Wortel, R. (2005).
894 Nappe stacking resulting from subduction of oceanic and continental lithosphere below Greece.
895 *Geology*, (4), 325–328. <https://doi.org/10.1130/G20878.1>
- 896 van Hinsbergen, D. J. J., Lippert, P. C., Dupont-Nivet, G., McQuarrie, N., Doubrovine, P. V.,
897 Spakman, W., & Torsvik, T. H. (2012). Greater India Basin hypothesis and a two-stage
898 Cenozoic collision between India and Asia. *Proceedings of the National Academy of Sciences*,
899 *109*(20), 7659–7664. <https://doi.org/10.1073/pnas.1117262109>
- 900 van Hinsbergen, D. J. J., Lippert, P. C., Li, S., Huang, W., Advokaat, E. L., & Spakman, W. (2019).

901 Tectonophysics Reconstructing Greater India : Paleogeographic , kinematic , and geodynamic
902 perspectives. *Tectonophysics*, (May 2017), 0–1. <https://doi.org/10.1016/j.tecto.2018.04.006>

903 van Hinsbergen, D. J., Steinberger, B., & Doubrovine, P. V. (2011). Acceleration and deceleration of
904 India - Asia convergence since the Cretaceous : Roles of mantle plumes and continental
905 collision. *Journal of Geophysical Research*, *116*, 1–20. <https://doi.org/10.1029/2010JB008051>

906 van Hinsbergen, Douwe J.J., Lippert, P. C., Li, S., Huang, W., Advokaat, E. L., & Spakman, W.
907 (2019). Reconstructing Greater India: Paleogeographic, kinematic, and geodynamic
908 perspectives. *Tectonophysics*, *760*(May 2017), 69–94.
909 <https://doi.org/10.1016/j.tecto.2018.04.006>

910 van Hinsbergen, Douwe J.J., Spakman, W., de Boorder, H., van Dongen, M., Jowitt, S. M., & Mason,
911 P. R. D. (2020). Arc-Type Magmatism Due to Continental-Edge Plowing Through Ancient
912 Subduction-Enriched Mantle. *Geophysical Research Letters*, *47*(9), 1–11.
913 <https://doi.org/10.1029/2020GL087484>

914 van Hinsbergen, Douwe J J, & Schouten, T. L. A. (2021). Deciphering paleogeography from orogenic
915 architecture : constructing orogens in a future supercontinent as thought experiment. *American*
916 *journal of science*, *321*, 955–1031. <https://doi.org/10.2475/06.2021.09>

917 van Hinsbergen, Douwe J J, Kapp, P., Nivet, G. D., Lippert, P. C., Decelles, P. G., & Torsvik, T. H.
918 (2011). Restoration of Cenozoic deformation in Asia and the size of Greater India. *Tectonics*,
919 *30*, 1–31. <https://doi.org/10.1029/2011TC002908>

920 Hinsbergen, Douwe J J Van, Lippert, P. C., Dupont-nivet, G., & Mcquarrie, N. (2012). Greater India
921 Basin hypothesis and a two-stage Cenozoic collision between India and Asia, *109*(20).
922 <https://doi.org/10.1073/pnas.1117262109>

923 Hodges, K. V. (2000). Tectonics of the Himalaya and Southern Tibet from two perspectives. *Bulletin*
924 *of the Geological Society of America*, *112*(3), 324–350. [https://doi.org/10.1130/0016-](https://doi.org/10.1130/0016-7606(2000)112<324:TOTHAS>2.0.CO;2)
925 [7606\(2000\)112<324:TOTHAS>2.0.CO;2](https://doi.org/10.1130/0016-7606(2000)112<324:TOTHAS>2.0.CO;2)

926 Hu, X., Garzanti, E., Wang, J., Huang, W., An, W., & Webb, A. (2016). The timing of India-Asia
927 collision onset – Facts , theories , controversies. *Earth Science Reviews*, *160*, 264–299.
928 <https://doi.org/10.1016/j.earscirev.2016.07.014>

929 Huang, J., & Zhao, D. (2006). High-resolution mantle tomography of China and surrounding regions.
930 *Journal of Geophysical Research*, *111*(March), 1–21. <https://doi.org/10.1029/2005JB004066>

931 Huang, W., Hinsbergen, D. J. J. Van, Maffione, M., Orme, D. A., Dupont-nivet, G., Guilmette, C., et
932 al. (2015). Lower Cretaceous Xigaze ophiolites formed in the Gangdese forearc : Evidence from

- 933 paleomagnetism , sediment provenance , and stratigraphy. *Earth and Planetary Science Letters*,
934 415, 142–153. <https://doi.org/10.1016/j.epsl.2015.01.032>
- 935 van Hunen, J., & Allen, M. B. (2011). Continental collision and slab break-off: A comparison of 3-D
936 numerical models with observations. *Earth and Planetary Science Letters*, 302(1–2), 27–37.
937 <https://doi.org/10.1016/j.epsl.2010.11.035>
- 938 Ingalls, M., Rowley, D. B., Currie, B., & Colman, A. S. (2016). Large-scale subduction of continental
939 crust implied by India-Asia mass-balance calculation. *Nature Geoscience*, 9(11), 848–853.
940 <https://doi.org/10.1038/ngeo2806>
- 941 Jagoutz, O., Royden, L., Holt, A. F., & Becker, T. W. (2015). Anomalously fast convergence of India
942 and Eurasia caused by double subduction, 8(May). <https://doi.org/10.1038/NGEO2418>
- 943 Kapp, P., & Decelles, P. G. (2019). Mesozoic–Cenozoic geological evolution of the Himalayan-
944 Tibetan orogen and working tectonic hypotheses. *American Journal of Science*, 319(3), 159–
945 254. <https://doi.org/10.2475/03.2019.01>
- 946 Kapp, P., Yin, A., Harrison, T. M., & Ding, L. (2005). Cretaceous-Tertiary shortening , basin
947 development , and volcanism in central Tibet. *Geological Society of America Bulletin*, 117(7),
948 865–878. <https://doi.org/10.1130/B25595.1>
- 949 Khan, I. H., & Clyde, W. C. (2013). Lower Paleogene Tectonostratigraphy of Balochistan: Evidence
950 for Time-Transgressive Late Paleocene-Early Eocene Uplift. *Geosciences*, 3(5), 466–501.
951 <https://doi.org/10.3390/geosciences3030466>
- 952 Kohn, M. J., Parkinson, C. D., Kohn, M. J., & Parkinson, C. D. (2002). Petrologic case for Eocene
953 slab breakoff during the Indo-Asian collision. *Geology*, 30(7), 591–594.
954 [https://doi.org/10.1130/0091-7613\(2002\)030<0591](https://doi.org/10.1130/0091-7613(2002)030<0591)
- 955 Kopp, C., Fruehn, J., Flueh, E. R., Reichert, C., Kukowski, N., Bialas, J., & Klaeschen, D. (2000).
956 Structure of the makran subduction zone from wide-angle and reflection seismic data.
957 *Tectonophysics*, 329(1–4), 171–191. [https://doi.org/10.1016/S0040-1951\(00\)00195-5](https://doi.org/10.1016/S0040-1951(00)00195-5)
- 958 Kufner, S. K., Schurr, B., Haberland, C., Zhang, Y., Saul, J., Ischuk, A., & Oimahmadov, I. (2017).
959 Zooming into the Hindu Kush slab break-off: A rare glimpse on the terminal stage of
960 subduction. *Earth and Planetary Science Letters*, 461(October 2015), 127–140.
961 <https://doi.org/10.1016/j.epsl.2016.12.043>
- 962 Kufner, S. K., Kakar, N., Bezada, M., Bloch, W., Metzger, S., Yuan, X., et al. (2021). The Hindu
963 Kush slab break-off as revealed by deep structure and crustal deformation. *Nature*
964 *Communications*, 12(1), 1–11. <https://doi.org/10.1038/s41467-021-21760-w>

- 965 van de Lagemaat, S. H. A., van Hinsbergen, D. J. J., Boschman, L. M., Kamp, P. J. J., & Spakman,
966 W. (2018). Southwest Pacific Absolute Plate Kinematic Reconstruction Reveals Major Cenozoic
967 Tonga-Kermadec Slab Dragging. *Tectonics*, 37(8), 2647–2674.
968 <https://doi.org/10.1029/2017TC004901>
- 969 Lallemand, S., Heuret, A., Faccenna, C., & Funiciello, F. (2008). Subduction dynamics as revealed by
970 trench migration. *Tectonics*, 27(September 2007), 1–15. <https://doi.org/10.1029/2007TC002212>
- 971 Lee, C., & King, S. D. (2011). Dynamic buckling of subducting slabs reconciles geological and
972 geophysical observations. *Earth and Planetary Science Letters*, 312(3–4), 360–370.
973 <https://doi.org/10.1016/j.epsl.2011.10.033>
- 974 Lee, H., Chung, S., Lo, C., Ji, J., Lee, T., Qian, Q., & Zhang, Q. (2009). Tectonophysics Eocene
975 Neotethyan slab breakoff in southern Tibet inferred from the Linzizong volcanic record.
976 *Tectonophysics*, 477(1–2), 20–35. <https://doi.org/10.1016/j.tecto.2009.02.031>
- 977 Li, C., & Hilst, R. D. Van Der. (2010). Structure of the upper mantle and transition zone beneath
978 Southeast Asia from travelttime tomography, 115, 1–19. <https://doi.org/10.1029/2009JB006882>
- 979 Li, C., Hilst, R. D. Van Der, Meltzer, A. S., & Engdahl, E. R. (2008). Subduction of the Indian
980 lithosphere beneath the Tibetan Plateau and Burma. *Earth and Planetary Science Letters*, 274,
981 157–168. <https://doi.org/10.1016/j.epsl.2008.07.016>
- 982 Li, S., Yin, C., Guilmette, C., Ding, L., & Zhang, J. (2019). Birth and demise of the Bangong-Nujiang
983 Tethyan Ocean : A review from the Gerze area of central Tibet. *Earth-Science Reviews*,
984 198(April), 102907. <https://doi.org/10.1016/j.earscirev.2019.102907>
- 985 Li, Zhen, Qiu, J., & Yang, X. (2014). Earth-Science Reviews A review of the geochronology and
986 geochemistry of Late Yanshanian (Cretaceous) plutons along the Fujian coastal area of
987 southeastern China : Implications for magma evolution related to slab break-off and rollback in
988 the Cretaceous. *Earth Science Reviews*, 128, 232–248.
989 <https://doi.org/10.1016/j.earscirev.2013.09.007>
- 990 Li, Zhenyu, Ding, L., Lippert, P. C., Song, P., Yue, Y., & Hinsbergen, D. J. J. Van. (2016).
991 Paleomagnetic constraints on the Mesozoic drift of the Lhasa terrane (Tibet) from Gondwana
992 to Eurasia. *Geology*, 44(9), 727–730. <https://doi.org/10.1130/G38030.1>
- 993 Lippert, P. C., Van Hinsbergen, D. J. J., & Dupont-Nivet, G. (2014). Early Cretaceous to present
994 latitude of the central proto-Tibetan Plateau: A paleomagnetic synthesis with implications for
995 Cenozoic tectonics, paleogeography, and climate of Asia. *Special Paper of the Geological*
996 *Society of America*, 507, 1–21. [https://doi.org/10.1130/2014.2507\(01\)](https://doi.org/10.1130/2014.2507(01))

- 997 Lister, G., Kennett, B., Richards, S., & Forster, M. (2008). Boudinage of a stretching slablet
998 implicated in earthquakes beneath the Hindu Kush. *Nature Geoscience*, 1(3), 196–201.
999 <https://doi.org/10.1038/ngeo132>
- 1000 Lithgow-bertelloni, C., & Richards, M. A. (1998a). The Dynamics Of Cenozoic And Mesozoic
1001 Motions. *Reviews of Geophysics*, 36(97), 27–78.
- 1002 Lithgow-bertelloni, C., & Richards, M. A. (1998b). The Dynamics Of Cenozoic And Mesozoic
1003 Motions. *Reviews of Geophysics*, (97), 27–78.
- 1004 Luo, A. B., & Fan, J. J. (2020). Aptian Flysch in Central Tibet : Constraints on the Timing of Closure
1005 of the Bangong - Nujiang Tethyan Ocean. *Tectonics*, 39. <https://doi.org/10.1029/2020TC006198>
- 1006 Magni, V., Allen, M. B., Hunen, J. Van, & Bouilhol, P. (2017). Continental underplating after slab
1007 break-off. *Earth and Planetary Science Letters*, 474, 59–67.
1008 <https://doi.org/10.1016/j.epsl.2017.06.017>
- 1009 Maheo, G., Guillot, S., Blichert-toft, J., Rolland, Y., & Pe, A. (2002). A slab breakoff model for the
1010 Neogene thermal evolution of South Karakorum and South Tibet. *Earth and Planetary Science
1011 Letters*, 195.
- 1012 Martin, C. R., Jagoutz, O., Upadhyay, R., Royden, L. H., Eddy, M. P., Bailey, E., et al. (2020).
1013 Paleocene latitude of the Kohistan – Ladakh arc indicates multistage India – Eurasia collision.
1014 *PNAS*, 117(47). <https://doi.org/10.1073/pnas.2009039117>
- 1015 Maury, C., Coulon, C., Megartsi, M., Fourcade, S., Louni-hacini, A., Cotten, J., et al. (2002). Post-
1016 collisional transition from calc-alkaline to alkaline volcanism during the Neogene in Oranie (
1017 Algeria): magmatic expression of a slab breakoff. *LITHOS*, 62, 87–110.
- 1018 van der Meer, D. G., van Hinsbergen, D. J. J., & Spakman, W. (2018). Atlas of the underworld: Slab
1019 remnants in the mantle, their sinking history, and a new outlook on lower mantle viscosity.
1020 *Tectonophysics*, 723(June 2017), 309–448. <https://doi.org/10.1016/j.tecto.2017.10.004>
- 1021 Van Der Meer, D. G., Spakman, W., Van Hinsbergen, D. J. J., Amaru, M. L., & Torsvik, T. H.
1022 (2010). Towards absolute plate motions constrained by lower-mantle slab remnants. *Nature
1023 Geoscience*, 3(1), 36–40. <https://doi.org/10.1038/ngeo708>
- 1024 Van Der Meer, D. G., Zeebe, R. E., Hinsbergen, D. J. J. Van, Sluijs, A., & Spakman, W. (2014). Plate
1025 tectonic controls on atmospheric CO₂ levels since the Triassic. *PNAS*, 111(12).
1026 <https://doi.org/10.1073/pnas.1315657111>
- 1027 Meulen, M. J. Van Der, Meulenkamp, J. E., & Wortel, M. J. R. (1998). Lateral shifts of Apenninic
1028 foredeep depocentres reflecting detachment of subducted lithosphere. *Earth and Planetary*

- 1029 *Science Letters*, 154, 203–219.
- 1030 Miller, M. S., Gorbato, A., & Kennett, B. L. N. (2005). Heterogeneity within the subducting Pacific
1031 slab beneath the Izu-Bonin-Mariana arc: Evidence from tomography using 3D ray tracing
1032 inversion techniques. *Earth and Planetary Science Letters*, 235(1–2), 331–342.
1033 <https://doi.org/10.1016/j.epsl.2005.04.007>
- 1034 Molnar, P., & Stock, J. M. (2009). Slowing of India’s convergence with Eurasia since 20 Ma and its
1035 implications for Tibetan mantle dynamics. *Tectonics*, 28(3), 1–11.
1036 <https://doi.org/10.1029/2008TC002271>
- 1037 Molnar, P., & tapponnier, P. (1975). Cenozoic Tectonics of Asia: Effects of a Continental Collision.
1038 *Science*, 189(4201), 419–426.
- 1039 Morley, C. K., & Arboit, F. (2019). Dating the onset of motion on the Sagaing fault : Evidence from
1040 detrital zircon and titanite U-Pb geochronology from the North Minwun Basin , Myanmar,
1041 47(6), 581–585.
- 1042 Murphy, M. A., Harrison, T. M., Wang, X., & Zhou, X. (1997). Did the Indo-Asian collision alone
1043 create the Tibetan plateau ? *Geology*, 25(8), 719–722.
- 1044 Nábelek, J., Hetényi, G., Vergne, J., Sapkot, S., Kafle, B., Jiang, M., et al. (2009). Underplating in the
1045 Himalaya-Tibet Collision Zone Revealed by the Hi-CLIMB Experiment Underplating in the
1046 Himalaya-Tibet Collision Zone Revealed by the Hi-CLIMB Experiment. *Science*, 325(October).
1047 <https://doi.org/10.1126/science.1167719>
- 1048 Najman, Y., Appel, E., Fadel, M. B., Bown, P., Carter, A., Garzanti, E., et al. (2010). Timing of India
1049 - Asia collision : Geological , biostratigraphic , and palaeomagnetic constraints. *Journal of*
1050 *Geophysical Research*, 115(B12416), 1–18. <https://doi.org/10.1029/2010JB007673>
- 1051 Negredo, A. M., Replumaz, A., Villaseñor, A., & Guillot, S. (2007). Modeling the evolution of
1052 continental subduction processes in the Pamir – Hindu Kush region. *Earth and Planetary*
1053 *Science Letters*, 259, 212–225. <https://doi.org/10.1016/j.epsl.2007.04.043>
- 1054 Ninkabou, D., Agard, P., Nielsen, C., Smit, J., & Gorini, C. (2021). Structure of the offshore obducted
1055 Oman margin: emplacement of Semail ophiolite and role of tectonic inheritance. *Journal of*
1056 *Geophysical Research Solid Earth*, 126(2). <https://doi.org/10.1029/2020JB020187>
- 1057 Parsons, A. J., Hosseini, K., Palin, R., & Sigloch, K. (2020). Geological, geophysical and plate
1058 kinematic constraints for models of the India-Asia collision and the post-Triassic central Tethys
1059 oceans. *Earth-Science Reviews*, 202(January), 103084.
1060 <https://doi.org/10.1016/j.earscirev.2020.103084>

- 1061 Parsons, A. J., Sigloch, K., & Hosseini, K. (2021). Australian plate subduction is responsible for
1062 northward motion of the India- Asia collision zone and ~ 1000 km lateral migration of the Indian
1063 slab. *Geophysical Research Letters*, 48(18).
- 1064 Patriat, P., & Achache, J. (1984). India-Eurasia collision chronology has implications for crustal
1065 shortening and driving mechanism of plates. *Nature*.
- 1066 Plunder, A., Bandyopadhyay, D., Ganerød, M., & Advokaat, E. L. (2020). History of Subduction
1067 Polarity Reversal During Arc - Continent Collision : Constraints From the Andaman Ophiolite
1068 and its Metamorphic Sole. *Tectonics*, 39, 1–24. <https://doi.org/10.1029/2019TC005762>
- 1069 Regard, V., Faccenna, C., Bellier, O., & Martinod, J. (2008). Laboratory experiments of slab break-
1070 off and slab dip reversal : insight into the Alpine Oligocene reorganization. *Terra Nova*, 20,
1071 267–273. <https://doi.org/10.1111/j.1365-3121.2008.00815.x>
- 1072 Replumaz, Negredo, A. M., Guillot, S., & Villaseñor, A. (2010). Multiple episodes of continental
1073 subduction during India/Asia convergence: Insight from seismic tomography and tectonic
1074 reconstruction. *Tectonophysics*, 483(1–2), 125–134. <https://doi.org/10.1016/j.tecto.2009.10.007>
- 1075 Replumaz, A., & Tapponnier, P. (2003). Reconstruction of the deformed collision zone Between India
1076 and Asia by backward motion of lithospheric blocks. *Journal of Geophysical Research: Solid
1077 Earth*, 108(B6). <https://doi.org/10.1029/2001jb000661>
- 1078 Replumaz, Anne, Káráson, H., van der Hilst, R. D., Besse, J., & Tapponnier, P. (2004). 4-D evolution
1079 of SE Asia's mantle from geological reconstructions and seismic tomography. *Earth and
1080 Planetary Science Letters*, 221(1–4), 103–115. [https://doi.org/10.1016/S0012-821X\(04\)00070-6](https://doi.org/10.1016/S0012-821X(04)00070-6)
- 1081 Replumaz, Anne, Guillot, S., Villaseñor, A., & Negredo, A. M. (2013). Amount of Asian lithospheric
1082 mantle subducted during the India / Asia collision. *Gondwana Research*, 24(3–4), 936–945.
1083 <https://doi.org/10.1016/j.gr.2012.07.019>
- 1084 Replumaz, Anne, Capitanio, F. A., Guillot, S., Negredo, A. M., & Villaseñor, A. (2014). The coupling
1085 of Indian subduction and Asian continental tectonics. *Gondwana Research*, 26(2), 608–626.
1086 <https://doi.org/10.1016/j.gr.2014.04.003>
- 1087 Richards, M. A., & Engebretson, D. C. (1990). Large-scale mantle convection and the history of
1088 subduction, 4, 437–440.
- 1089 Rodriguez, M., Chamot-rooke, N., Huchon, P., & Fournier, M. (2014). Tectonics of the Dalrymple
1090 Trough and uplift of the Murray Ridge (NW Indian Ocean). *Tectonophysics*, (October 2017).
1091 <https://doi.org/10.1016/j.tecto.2014.08.001>
- 1092 Royden, L. H. (1993). Evolution Of Retreating Subduction Boundaries Formed During Continental

- 1093 Collision, *12*(3), 629–638.
- 1094 Royden, L. H., Burchfiel, B. C., & Hilst, R. D. Van Der. (2008). of the Tibetan Plateau. *Science*,
1095 *321*(August), 1054–1058.
- 1096 Schellart, W. P. (2008). Subduction zone trench migration: Slab driven or overriding-plate-driven?
1097 *Physics of the Earth and Planetary Interiors*, *170*(1–2), 73–88.
1098 <https://doi.org/10.1016/j.pepi.2008.07.040>
- 1099 Schellart, W. P., & Spakman, W. (2015). Australian plate motion and topography linked to fossil New
1100 Guinea slab below Lake Eyre. *Earth and Planetary Science Letters*, *421*, 107–116.
1101 <https://doi.org/10.1016/j.epsl.2015.03.036>
- 1102 Schepers, G., Van Hinsbergen, D. J. J., Spakman, W., Kosters, M. E., Boschman, L. M., &
1103 McQuarrie, N. (2017). South-American plate advance and forced Andean trench retreat as
1104 drivers for transient flat subduction episodes. *Nature Communications*, *8*(0316), 1–9.
1105 <https://doi.org/10.1038/ncomms15249>
- 1106 Sdrolias, M., & Müller, R. D. (2006). Controls on back-arc basin formation. *Geochemistry*,
1107 *Geophysics, Geosystems*, *7*(4). <https://doi.org/10.1029/2005GC001090>
- 1108 Shephard, G. E., Matthews, K. J., Hosseini, K., & Domeier, M. (2017). On the consistency of
1109 seismically imaged lower mantle slabs. *Scientific Reports*, *7*(1), 1–17.
1110 <https://doi.org/10.1038/s41598-017-11039-w>
- 1111 Sigloch, K., & Mihalynuk, M. G. (2013). Intra-oceanic subduction shaped the assembly of Cordilleran
1112 North America. *Nature*, *496*(7443), 50–56. <https://doi.org/10.1038/nature12019>
- 1113 Song, P., Ding, L., Li, Z., Lippert, P. C., & Yue, Y. (2017). An early bird from Gondwana:
1114 Paleomagnetism of Lower Permian lavas from northern Qiangtang (Tibet) and the geography of
1115 the Paleo-Tethys. *Earth and Planetary Science Letters*, *475*(October), 119–133.
1116 <https://doi.org/10.1016/j.epsl.2017.07.023>
- 1117 spakman, W., Wortel, M. J. R., & Vlaar, N. J. (1988). The Hellenic Subduction Zone: A Tomographic
1118 Image And Its Geodynamic Implications. *Geophysical Research Letters*, *15*(1), 60–63.
- 1119 Spakman, W., Chertova, M. V, Van Den Berg, A., & Van Hinsbergen, D. J. J. (2018). Puzzling
1120 features of western Mediterranean tectonics explained by slab dragging. *Nature Geoscience*,
1121 *11*(3), 211–216. <https://doi.org/10.1038/s41561-018-0066-z>
- 1122 Sperner, B., Lorenz, F., Bonjer, K., Hettel, S., Müller, B., & Wenzel, F. (2001). Slab break-off -
1123 Abrupt cut or gradual detachment? New insights from the Vrancea Region (SE Carpathians,
1124 Romania). *Terra Nova*, *13*(3), 172–179. <https://doi.org/10.1046/j.1365-3121.2001.00335.x>

- 1125 Torsvik, T. H., Van der Voo, R., Preeden, U., Mac Niocaill, C., Steinberger, B., Doubrovine, P. V., et
 1126 al. (2012). Phanerozoic Polar Wander, Palaeogeography and Dynamics. *Earth-Science Reviews*,
 1127 *114*(3–4), 325–368. <https://doi.org/10.1016/j.earscirev.2012.06.007>
- 1128 Torsvik, T. H., Voo, R. Van Der, Doubrovine, P. V, Burke, K., & Steinberger, B. (2014). Deep
 1129 mantle structure as a reference frame for movements in and on the Earth. *PNAS*, *111*(24).
 1130 <https://doi.org/10.1073/pnas.1318135111>
- 1131 Torsvik, T. H., Steinberger, B., & Shephard, G. E. (2019). Pacific - Panthalassic Reconstructions :
 1132 Overview , Errata and the Way Forward Geochemistry , Geophysics , Geosystems.
 1133 *Geochemistry Geophysics Geosystems*, *20*, 3659–3689. <https://doi.org/10.1029/2019GC008402>
- 1134 Vissers, R. L. M., van Hinsbergen, D. J. J., van der Meer, D. G., & Spakman, W. (2016). Cretaceous
 1135 slab break-off in the Pyrenees: Iberian plate kinematics in paleomagnetic and mantle reference
 1136 frames. *Gondwana Research*, *34*, 49–59. <https://doi.org/10.1016/j.gr.2016.03.006>
- 1137 Van Der Voo, R., Spakman, W., & Bijwaard, H. (1999). Tethyan subducted slabs under India. *Earth
 1138 and Planetary Science Letters*, *171*(1), 7–20. [https://doi.org/10.1016/S0012-821X\(99\)00131-4](https://doi.org/10.1016/S0012-821X(99)00131-4)
- 1139 Van Der Voo, R., Van Hinsbergen, D. J. J., Domeier, M., Spakman, W., & Torsvik, T. H. (2015).
 1140 Latest Jurassic-earliest Cretaceous closure of the Mongol-Okhotsk Ocean: A paleomagnetic and
 1141 seismological-tomographic analysis. *Special Paper of the Geological Society of America*,
 1142 *513*(June), 589–606. [https://doi.org/10.1130/2015.2513\(19\)](https://doi.org/10.1130/2015.2513(19))
- 1143 Westerweel, J., Roperch, P., Licht, A., Dupont-Nivet, G., Win, Z., Poblete, F., et al. (2019). Burma
 1144 Terrane part of the Trans-Tethyan arc during collision with India according to palaeomagnetic
 1145 data. *Nature Geoscience*, *12*(10), 863–868. <https://doi.org/10.1038/s41561-019-0443-2>
- 1146 Wortel, M. J. R., & Spakman, W. (1992). Structure and dynamic of subducted lithosphere in the
 1147 Mediterranean. *Proc. Kon. Ned. Akad. v. Wetensch*, *95*(3), 325–347.
- 1148 Wortel, M. J. R., & Spakman, W. (2000). Subduction and slab detachment in the Mediterranean-
 1149 Carpathian region. *Science*, *290*(5498), 1910–1917.
 1150 <https://doi.org/10.1126/science.290.5498.1910>
- 1151 Wu, J., Suppe, J., Lu, R., & Kanda, R. (2016). Philippine Sea and East Asian plate tectonics since 52
 1152 Ma constrained by new subducted slab reconstruction methods. *Journal of Geophysical
 1153 Research: Solid Earth*, *121*(6), 4670–4741. <https://doi.org/10.1002/2016JB012923>
- 1154 Yamini-Fard, F., Hatzfeld, D., Farahbod, A. M., Paul, A., & Mokhtari, M. (2007). The diffuse
 1155 transition between the Zagros continental collision and the Makran oceanic subduction (Iran):
 1156 microearthquake seismicity and crustal structure. *Geophysical Journal International*, *170*, 182–

- 1157 194. <https://doi.org/10.1111/j.1365-246X.2006.03232.x>
- 1158 Yin, A., & Harrison, T. M. (2000). Geologic Evolution Of The Himalayan - Tibetan Oogen. *Annu.*
1159 *Rev. Earth Planet. Sci*, 28, 211–80.
- 1160 Yoshioka, S., & Wortel, M. J. R. (1995). Three-dimensional numerical modeling of detachment of
1161 subducted lithosphere. *Journal of Geophysical Research*, 100(B10).
1162 <https://doi.org/10.1029/94jb01258>
- 1163 Yuan, C., Sun, M., Wilde, S., Xiao, W., Xu, Y., Long, X., & Zhao, G. (2010). Lithos Post-collisional
1164 plutons in the Balikun area , East Chinese Tianshan : Evolving magmatism in response to
1165 extension and slab break-off. *LITHOS*, 119(3–4), 269–288.
1166 <https://doi.org/10.1016/j.lithos.2010.07.004>
- 1167 van de Zedde, D. M. A., & Wortel, M. J. R. (2001). Shallow slab detachment as a transient source of
1168 heat at midlithospheric depths. *Tectonics*, 20(6), 868–882.
1169 <https://doi.org/10.1029/2001TC900018>
- 1170 Zhao, D., & Ohtani, E. (2009). Deep slab subduction and dehydration and their geodynamic
1171 consequences : Evidence from seismology and mineral physics. *Gondwana Research*, 16(3–4),
1172 401–413. <https://doi.org/10.1016/j.gr.2009.01.005>
- 1173 Zhu, D., Wang, Q., Zhao, Z., Chung, S., Cawood, P. A., Niu, Y., et al. (2015). Magmatic record of
1174 India-Asia collision. *Nature Scientific Reports*, 1–9. <https://doi.org/10.1038/srep14289>
- 1175 Zhu, D., Li, S., Cawood, P. A., Wang, Q., Zhao, Z., Liu, S., & Wang, L. (2016). Assembly of the
1176 Lhasa and Qiangtang terranes in central Tibet by divergent double subduction. *LITHOS*, 245, 7–
1177 17. <https://doi.org/10.1016/j.lithos.2015.06.023>

1178

1179

1180

1181

1182

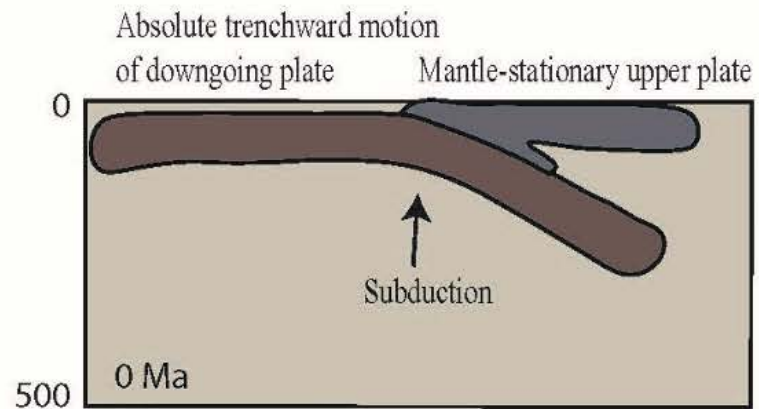
1183

1184

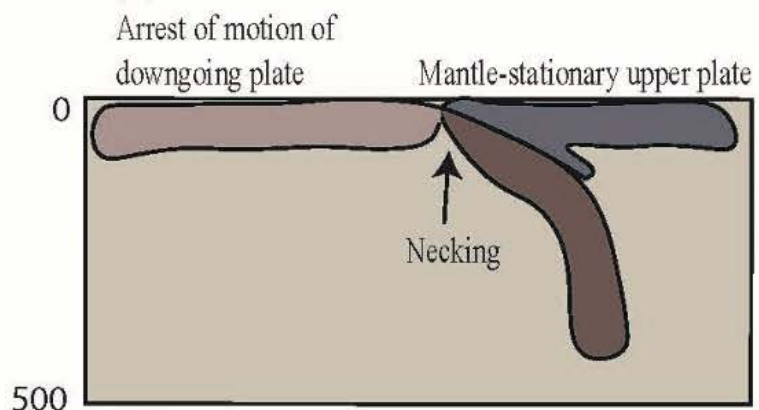
1185

1186

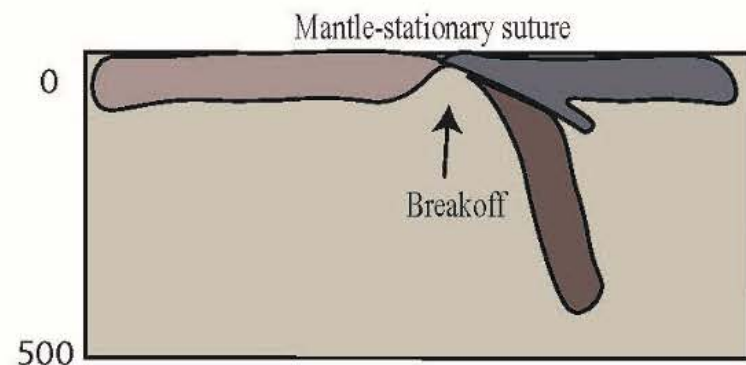
Conceptual model of slab break-off



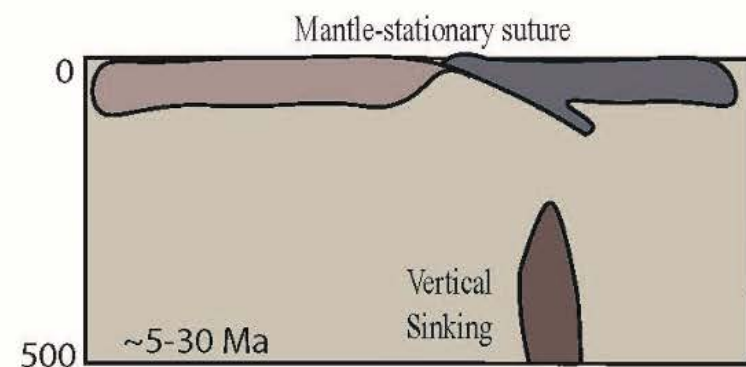
(a)



(b)



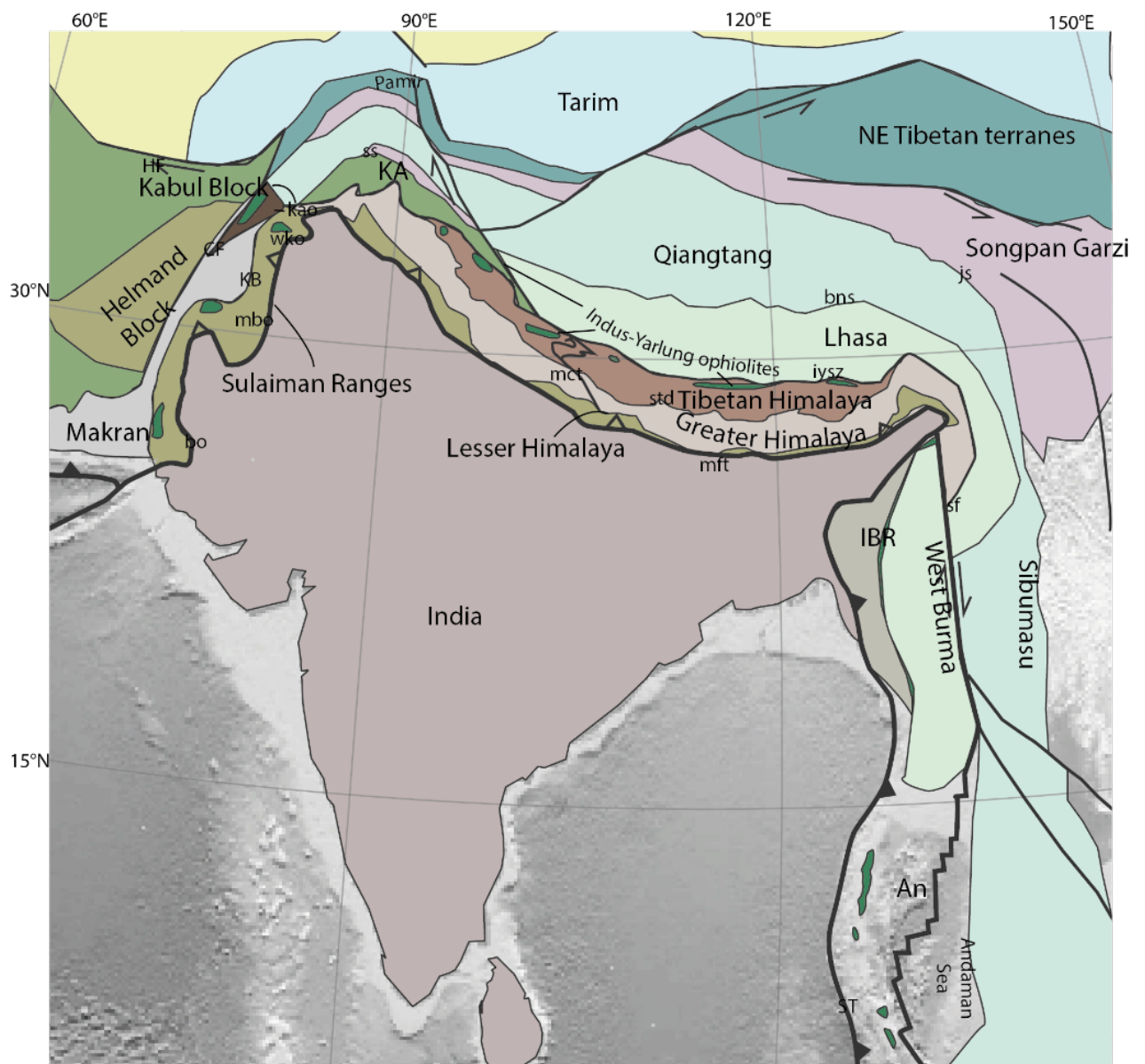
(c)



(d)

1188
1189
1190
1191
1192
1193
1194
1195
1196

Figure 1: Comparison of the shallow slab break off conceptual numerical model (a-d) (Duretz et al., 2011) vs proposed slab shear off model of Indian & Eurasian plate. It is observed that slab break off numerical models are different to reality (Static Trench vs Trench Advance). (a) represents the oceanic subduction, (b) represents continental collision, (c) represents necking and break off respectively (d) represents the post break off rebound.

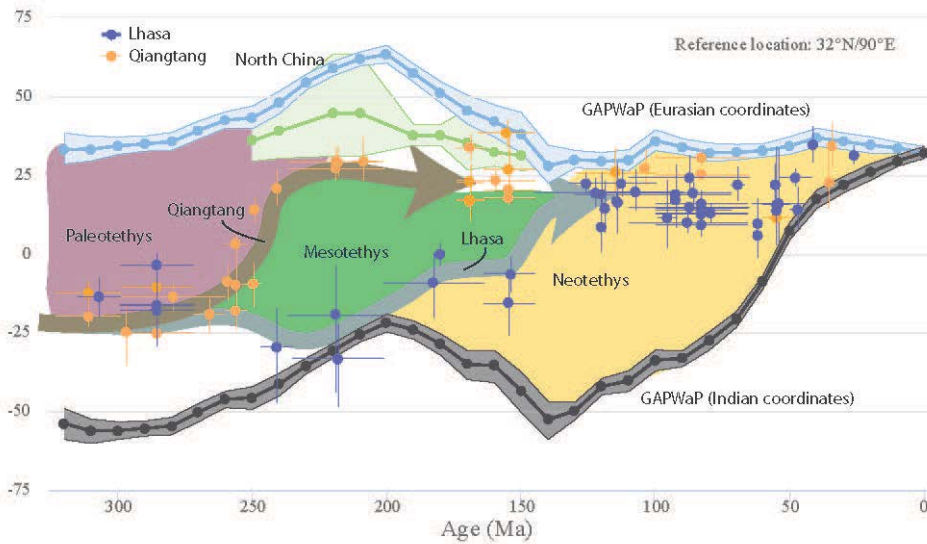


1197
1198
1199

Figure 2. Tectonic Map of the Asian-India collision region. Abbreviations are: An=Andaman Islands;; bns=Bangong-Nujiang Suture; bo=Bela Ophiolite; CF=Chaman Fault; HF=Herat Fault; MFT=Main

1200 Frontal Thrust; IBR=Indo-Burman Ranges; IYSZ=Indus-Yarlung Suture Zone; KA=Kohistan Arc;
 1201 kao=Kabul-Altinur Ophiolite; KB=Ka- tawaz Basin; js=Jinsha Suture; mbo=Muslim Bagh Ophiolite;
 1202 mct=Main Central Thrust; mft=Main Frontal Thrust; SF=Sagaing Fault; SS=Shyok Suture; ST=Sunda
 1203 Trench; std.=South Tibetan Detachment; wko=Waziristan-Khost Ophiolite.

1204

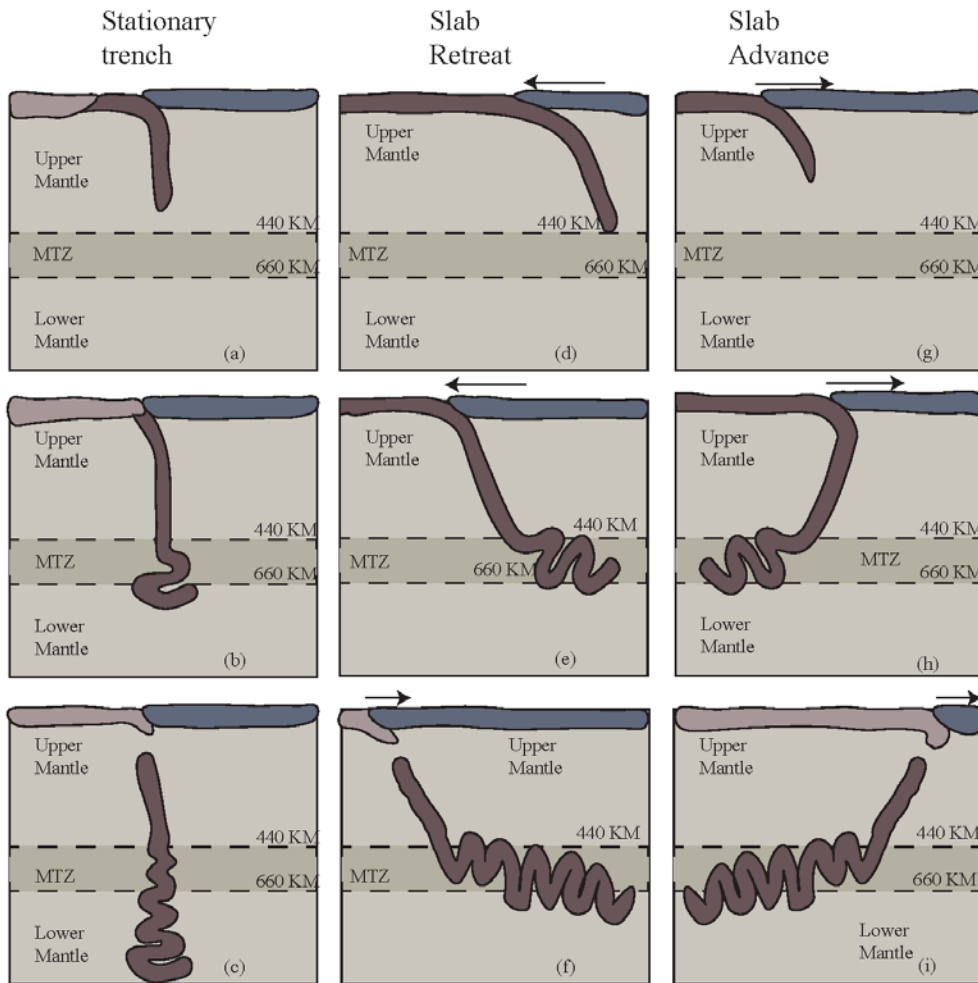


1205

1206 Figure 3. Paleolatitude curves for a reference point (32°N, 90°E). Each curve shows a paleolatitude
 1207 predicted for the reference point by the Global Apparent Polar Wander Path of Torsvik et al. (2012),
 1208 assuming the reference point was rigidly connected to Eurasia (blue curve), Lhasa (orange curve), and
 1209 India (black curve). Each curve indicate a lost ocean and relevant lithosphere in between and marked
 1210 with different colors.

1211

Slab shape as function of absolute slab and trench motion during subduction

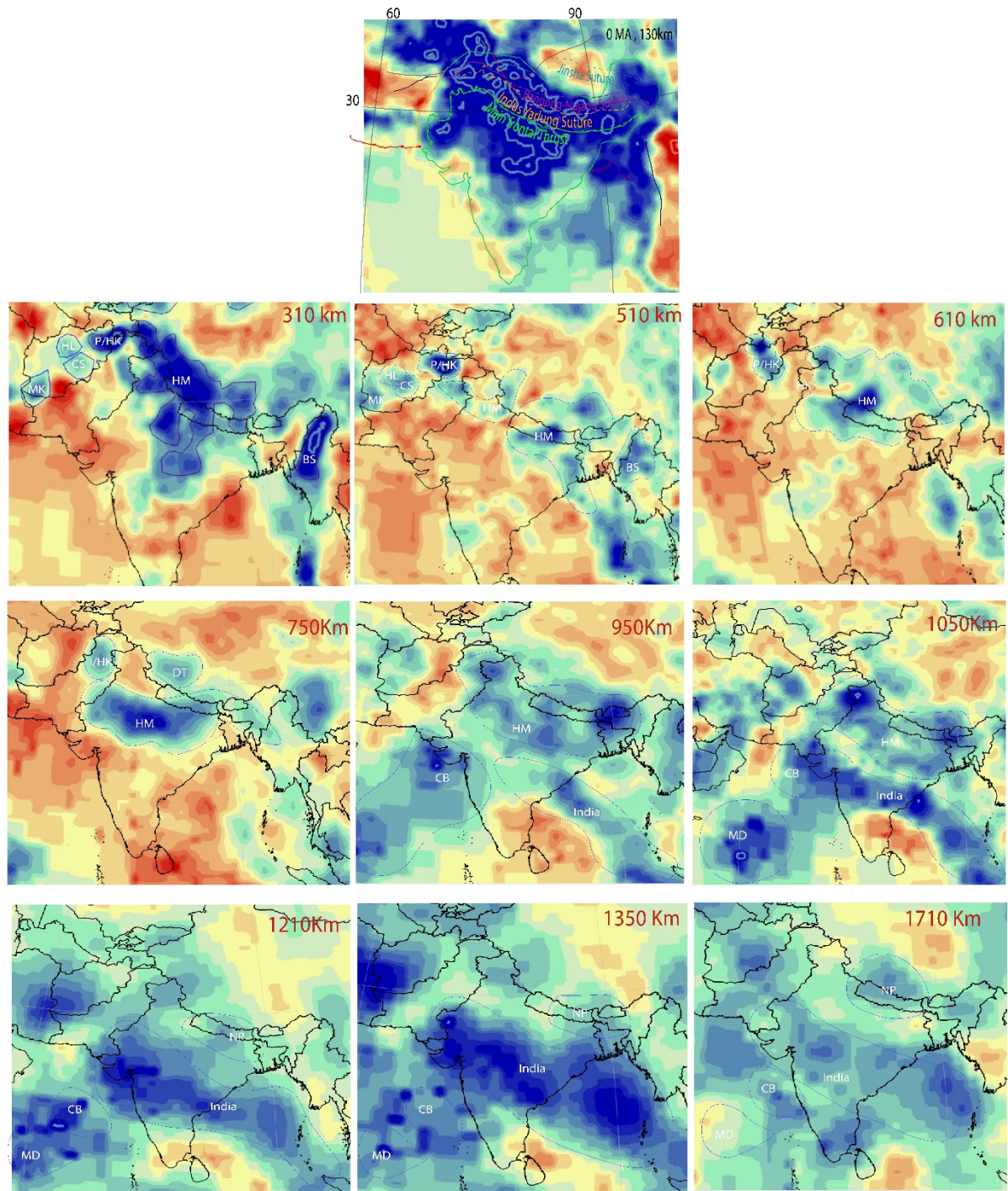


1212

1213 Figure 4: Conceptual models of the Slab detachment (g-i) as compared with existing models of slab
 1214 breakoff in various subduction scenarios(a-c, d-f) (Parsons et al., 2020). Proposed Trench Advance
 1215 model indicating trench moving forward and leaving detached slab behind in the mantle (g-l) oceanic
 1216 crust, continental crust and overriding plates are coloured in separate colours.

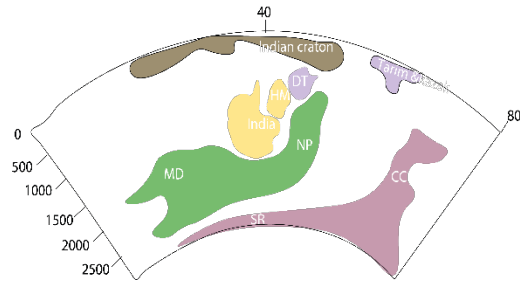
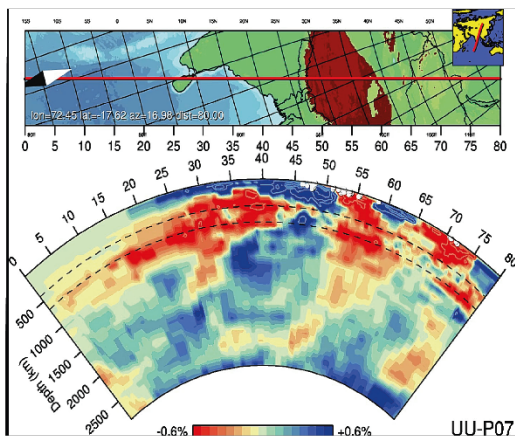
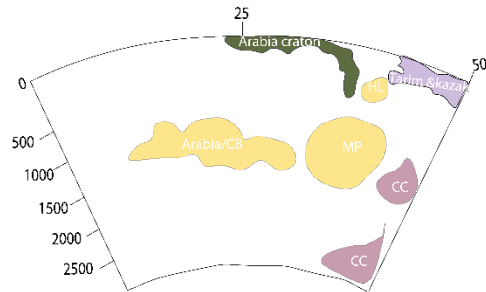
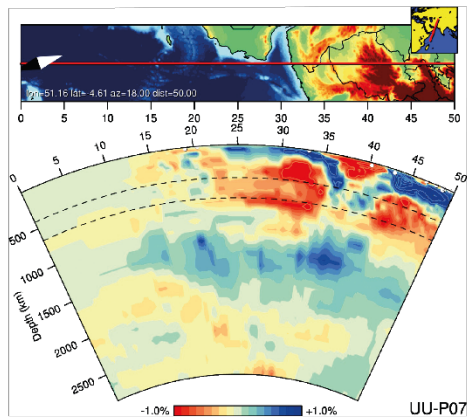
1217

1218



1219

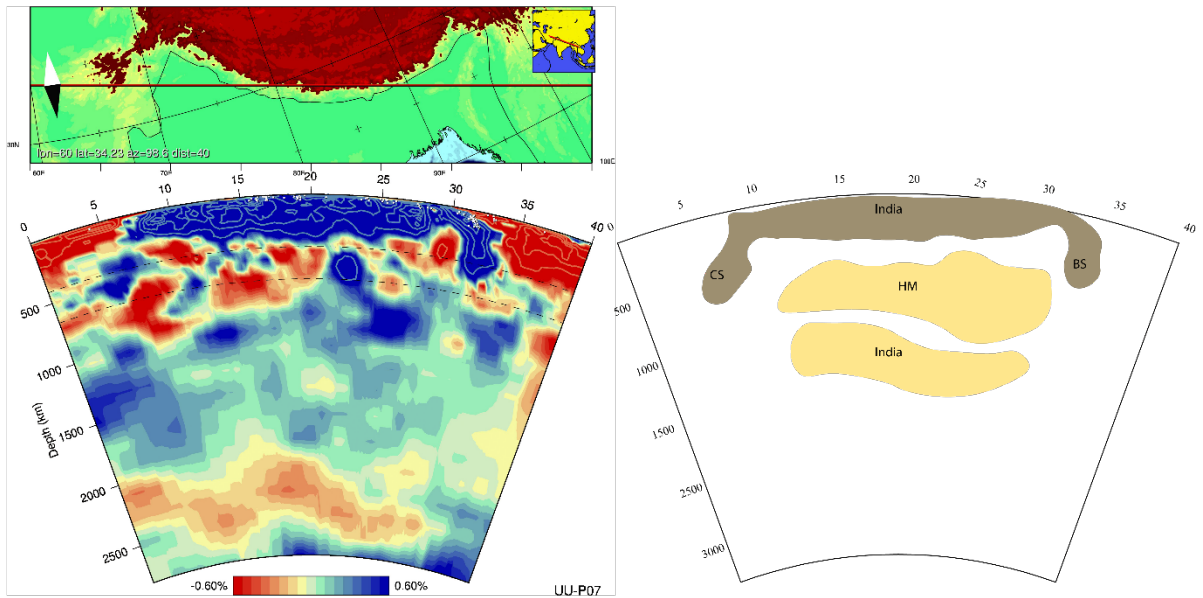
1220 Figure 5: Tomographic Horizontal sections indicating the relative positions and geometric variations
 1221 of anomalies. Hm: Himalaya Anomaly, India: India Anomaly, MD: Maldives anomaly, BS: Burma
 1222 Slab, CC: Central China anomaly, CS: Chaman Slab NP=Nepal anomaly, DT= Detached Tibet, Tarim
 1223 & Kazak= Tarim & Kazak Anomaly, Arabia/CB= Carlsberg anomaly, HL= Helmand anomaly, MK=
 1224 Makran anomaly . Line of section in shown in the inset map.



1225

1226 Figure 6: Cross section through the tomography model UU-P07. Labels display the positions of
 1227 anomalies. Hm: Himalaya Anomaly, India: India Anomaly, MD: Maldives anomaly, BS: Burma Slab,
 1228 CC Central China anomaly, NP=Nepal anomaly, DT= Detached Tibet, Tarim & Kazak= Tarim &
 1229 Kazak Anomaly, Arabia/CB= Carlsberg anomaly, HI= Helmand anomaly, MK= Makran anomaly,
 1230 SR= Sri Lanka Anomaly . Line of section in shown in the inset map.

1231

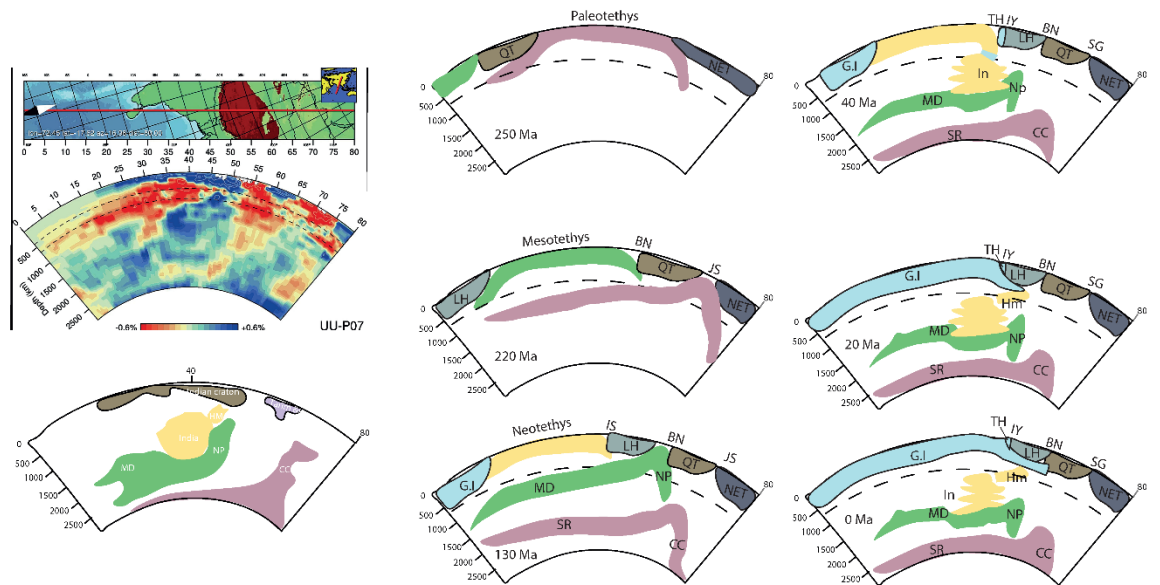


1232

1233 Figure 7: E-W Tomographic section through northern Indian plate. Oblique subduction is observed at
 1234 the western and eastern margin of Indian plate. BS=Burma Slab, CS= Chaman slab, HM= Himalaya
 1235 slab.

1236

1237



1238

1239 Figure 8: Interpreted models of the subducted slabs since 250 Ma and their comparison with the
 1240 reference tomographic interpretation (on left). At the present day configuration PaleoTethys slabs (pink)

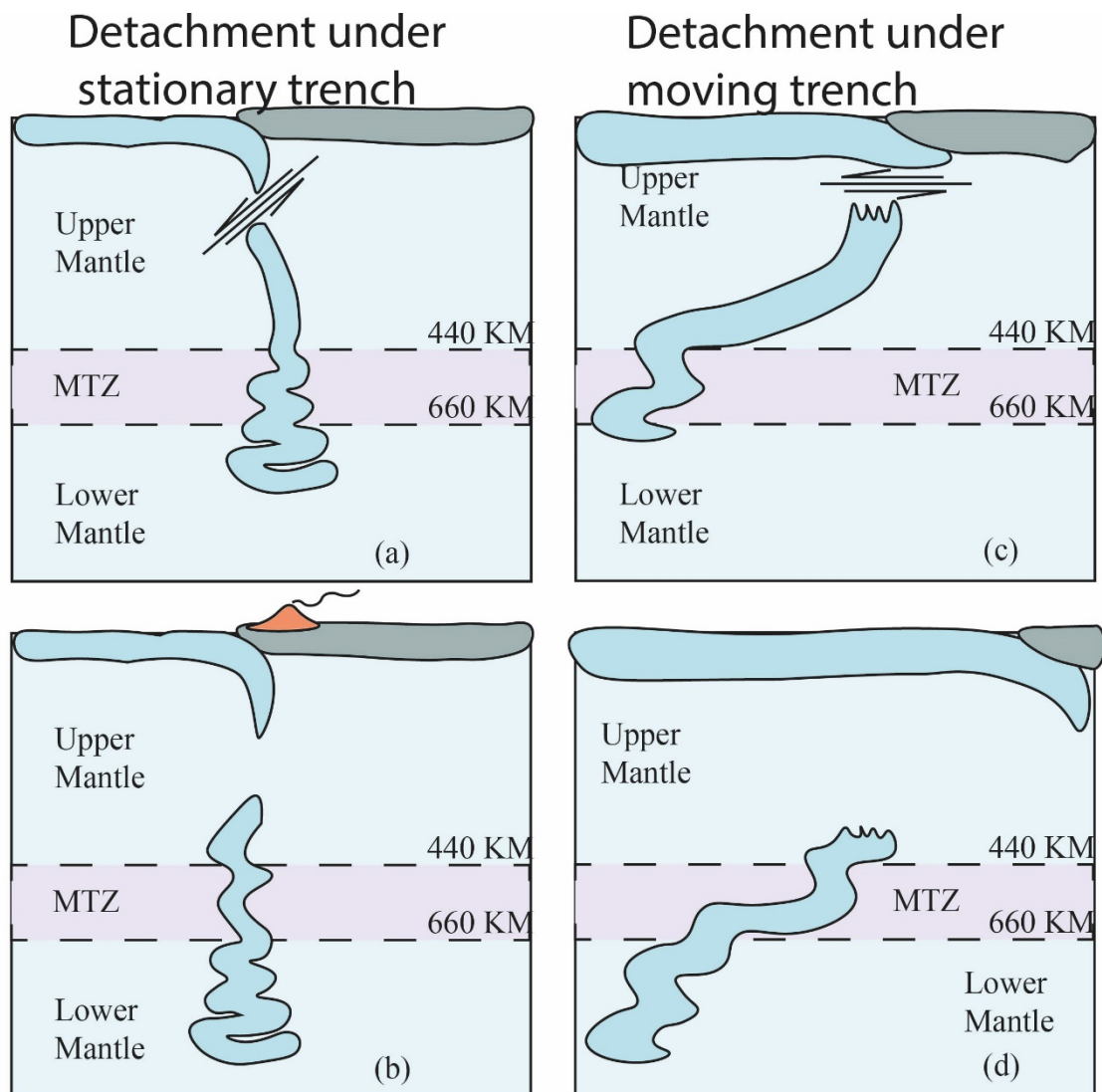
1241 can be found deep in the mantle at the Core mantle boundary, MesoTethys slabs (green) are just above
1242 followed by the Neo Tethys slabs (Yellow). Notice the trench advance during all the subduction
1243 scenarios.

1244

1245

1246

1247

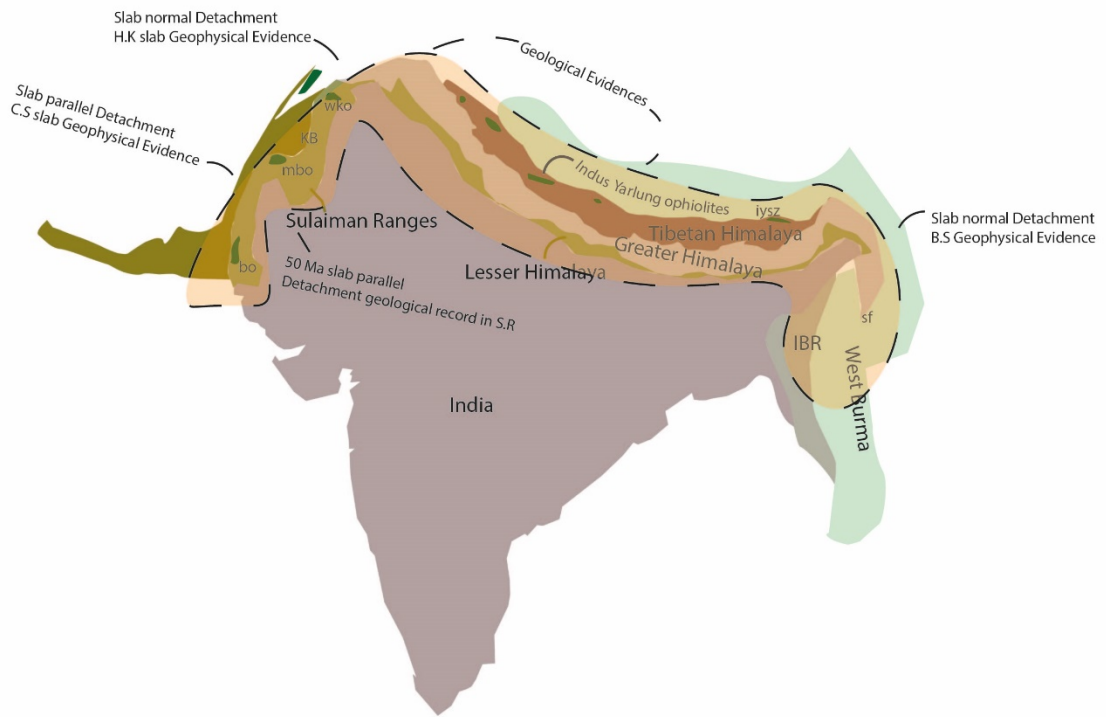


1248

1249

1250 Figure 9: Comparison of Detachment under stationary trench against Detachment under moving
1251 trench. Notice the sub vertical shear in the Detachment under stationary and the sub horizontal shear
1252 in case of Detachment under moving trench. Detachment under stationary is followed by the
1253 volcanism and Detachment under moving trench is followed by the trench advance resulting in
1254 possibly overturned slab.

1255



1256
 1257 Figure 10: Map indicating the future Geological and Geophysical learning opportunities in the study
 1258 area. Geological and Geophysical evidences can be compared to resolve the complex nature of
 1259 subduction during India- Asia collision.